11-20-2020

Study of Groundwater-Surface Water Interactions to Identify Potential Aquitard Breach Locations along the Wolf River, Tennessee

Sagar Pandit

STUDY OF GROUNDWATER-SURFACE WATER INTERACTIONS TO IDENTIFY POTENTIAL AQUITARD BREACH LOCATIONS ALONG THE WOLF RIVER, TENNESSEE

by

Sagar Pandit

A Thesis

Submitted in Partial Fulfillment of the

Requirements for the Degree of

Master of Science

Major: Civil Engineering

The University of Memphis

December 2020

ACKNOWLEDGMENTS

I would like to express my sincere appreciation to my advisor, Dr. Claudio Meier, who convincingly guided and encouraged me to be professional. The completion of this thesis would not have been possible without his continuous support and nurturing. I'm deeply indebted to Dr. Brian Waldron who continuously assisted this research with his ideas and visions. I would also like to express my inmost gratitude to Dr. Scott Schoefernacker, for his untiring support and guidance during field work, and to Dr. Daniel Larsen for his advice and comments to this work.

I would like to recognize the invaluable assistance that Rodrigo Villalpando-Vizcaíno provided me during this study. I am grateful to my fellow graduate students for their moral support and providing a helping hand during the demanding fieldwork days. Especial thanks the University of Memphis and the Center for Applied Earth Science and Engineering (CAESER) for the great opportunity they have provided to me. I would like to thank Memphis Light, Gas and Water (MLGW) for their support. Without their funding, this project could not have been possible.

Finally, I wish to acknowledge the support and great love of my family. They always encouraged me to do the right thing even when the road got tough.

PREFACE

This chapter has been formatted in the style of the *Journal of the American Water Resources Association* (JAWRA), to which the present work will be submitted for publication.

ABSTRACT

Inter-aquifer exchanges due to breaches in the confining clay layer can potentially contaminate the Memphis aquifer, as lesser-quality waters permeate from the unconfined aquifer. Losing river reaches could indicate breach locations, as these should depress water-table levels locally, resulting in downward vertical exchange fluxes (VEFs) along nearby streambeds. A spatial analysis of seepage meter measurements performed along the Wolf River identified three potentially losing sub-reaches, where VEFs were studied at a finer scale, using multiple point-scale methods. Results were mixed, displaying large spatial variability, possibly due to mismatches between the process and observation scales. Differential stream gaging was conducted to assess losses integrally over sub-reaches, confirming one losing location; however, comparing groundwater river stages suggested gaining conditions at this location. Pinpointing losing reaches using point-scale methods is difficult due to the disparity of scales. Effective methodologies are needed that comply with the scale of the problem.

TABLE OF CONTENTS

LIST OF FIGURES

LIST OF TABLES

Table Page

INTRODUCTION

Groundwater is a major source of water for domestic, municipal and industrial use in the United States, with an estimated use of 311.5 billion liters per day of fresh groundwater in 2015 (Dieter *et al.*, 2018). The growing use of groundwater has increased the vulnerability of aquifers to contamination, raising concerns about the need to protect groundwater from potential pollution sources, as is the case in Shelby County, Tennessee. The Memphis aquifer (the confined unit) is the primary source of drinking water for the Memphis metropolitan area, providing about 95% of the water used in the city (Graham and Parks, 1986; Parks and Carmichael, 1990). The Memphis aquifer is confined by the protective Upper Claiborne confining unit (UCCU), an extensive, thick clay layer that separates it from the overlying unconfined aquifer. An important issue is that there are discontinuities or breaches in the UCCU that allow for water exchange with the unconfined aquifer (Graham and Parks, 1986; Parks, 1990; Larsen *et al.*, 2003). This could potentially threaten the water quality of the Memphis aquifer due to downward migration of water from contaminated sites in Shelby County.

The Memphis aquifer, referred to as the "500-foot sand" in earlier studies (e.g., Nyman 1965), is a semi-confined aquifer which covers approximately 19166 km^2 in the Gulf Coastal Plain of western Tennessee (Parks and Carmichael, 1990). It is part of the Mississippi Embayment aquifer system which consists of very fine to very coarse sand of Cretaceous, Tertiary, and Quaternary ages, with individual aquifers ranging from 0 to 274 m in thickness (Graham and Parks, 1986; Parks, 1990). As described in Parks (1990) and many other works, the UCCU separates the Memphis aquifer from the overlying unconfined aquifer, whereas the Flour Island formation lies deeper, between the Memphis and the Fort Pillow aquifers, as shown in Figure 1.

In the Memphis area, the unconfined aquifer predominantly consists of alluvium and fluvial deposits (Graham and Parks, 1986). It used to be a source of water for many domestic, farm, and irrigation wells in the Memphis area, but due to the poor water quality, it is not in use as a major water source (Graham and Parks, 1986). The unconfined aquifer is recharged from infiltration and subsequent percolation of rainwater. It is hydrologically connected to the local streams and also gets some recharge from these watercourses during floods or high stage periods (Brahana and Broshears, 2001; Graham and Parks, 1986). The unconfined aquifer contributes a significant amount of water to streams in Shelby County, during low flow periods.

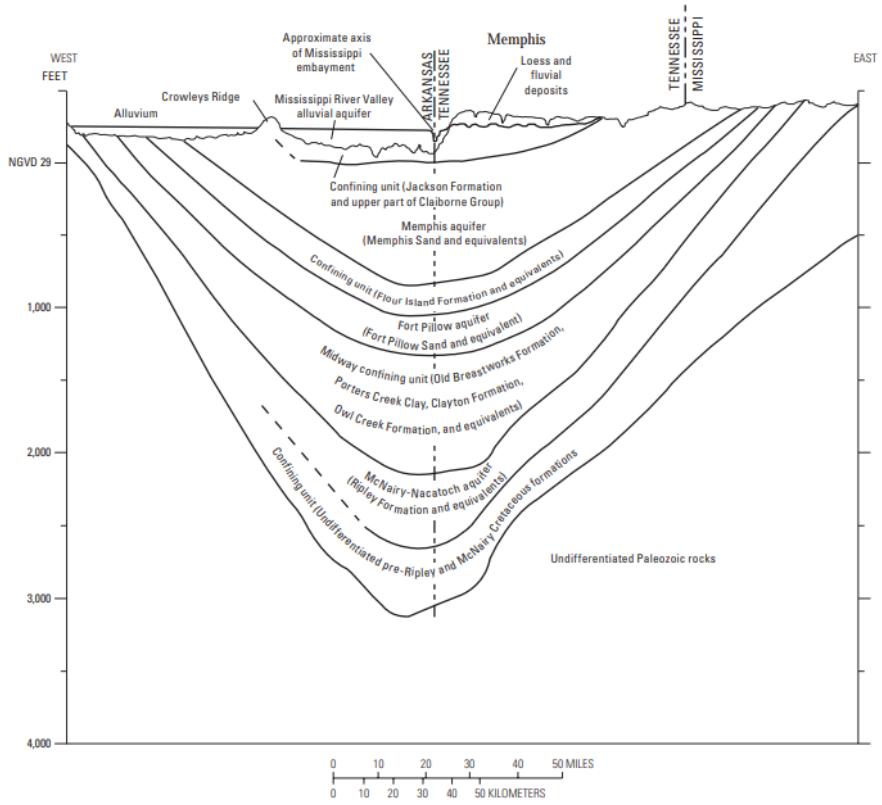

Figure 1. Cross-section of the Mississippi embayment stratigraphy (Source: Carmichael et al., 2018)

The UCCU consists of clay, silt, fine sand, and lignite. It has a significantly low hydraulic conductivity, that restricts inter-aquifer water exchange (Graham and Parks, 1986). Historically, the UCCU has been assumed to be of sufficiently thickness and impermeability

so as to protect the Memphis aquifer from contamination (Parks, 1990). But various studies since the 1960s suggest that there is exchange of water between the unconfined aquifer and the Memphis aquifer, due to discontinuities in this confining layer. The investigation of Graham and Parks (1986) indicates the presence of relatively recent water in the upper part of the Memphis aquifer, as well as recent precipitation water in the Memphis aquifer near the Sheahan well field, located in the Normal Station neighborhood of Memphis. Larsen et al. (2013) investigated the flow paths from Nonconnah Creek, a stream which flows through Memphis, to the Sheahan well field, through the study of stream discharge and hydraulic head data, tracer studies, and geochemical modeling. They concluded that some water flows from Nonconnah Creek to the unconfined aquifer, and ultimately to the Memphis aquifer in the Sheahan well field area. Larsen et al. (2016) also found the presence of relatively younger water (< 60 years) in the upper part of the Memphis aquifer, from age-dating of local production wells.

According to Criner et al. (1964), the upper confining unit is thin or absent in some places in the Memphis area, allowing for inter-aquifer exchange of water; this is also supported by more recent studies (Graham and Parks, 1986; Parks, 1990; Gentry *et al.*, 2006; Waldron *et al.*, 2009). Graham and Parks (1986) compiled and investigated isotope and geothermal data, water levels in the unconfined aquifer, as well as information from geophysical well logs. They concluded that there are at least four locations where the confining layer is thin or absent, providing their coordinates. Parks (1990) presents a map of the approximate distribution of breaches in the UCCU (Figure 2), obtained by investigating the thickness of the UCCU, anomalous depressions in the water table, tracer concentrations in water obtained from the Memphis aquifer, and series of discharge measurements in local streams during low flow conditions. Larsen (personal comm.) updated the map provided by Parks (1990) with information obtained from more recent studies. They classify breaches in

three categories: confirmed windows (breaches), probable windows, and potential windows, based on the amount of known information for each breach. Moreover, many other studies give information about anomalous depressions in the water table, which could signal the location of potential breaches (e.g., Narsimha, 2007; Bradshaw, 2011; Ogletree, 2016; Smith, 2018).

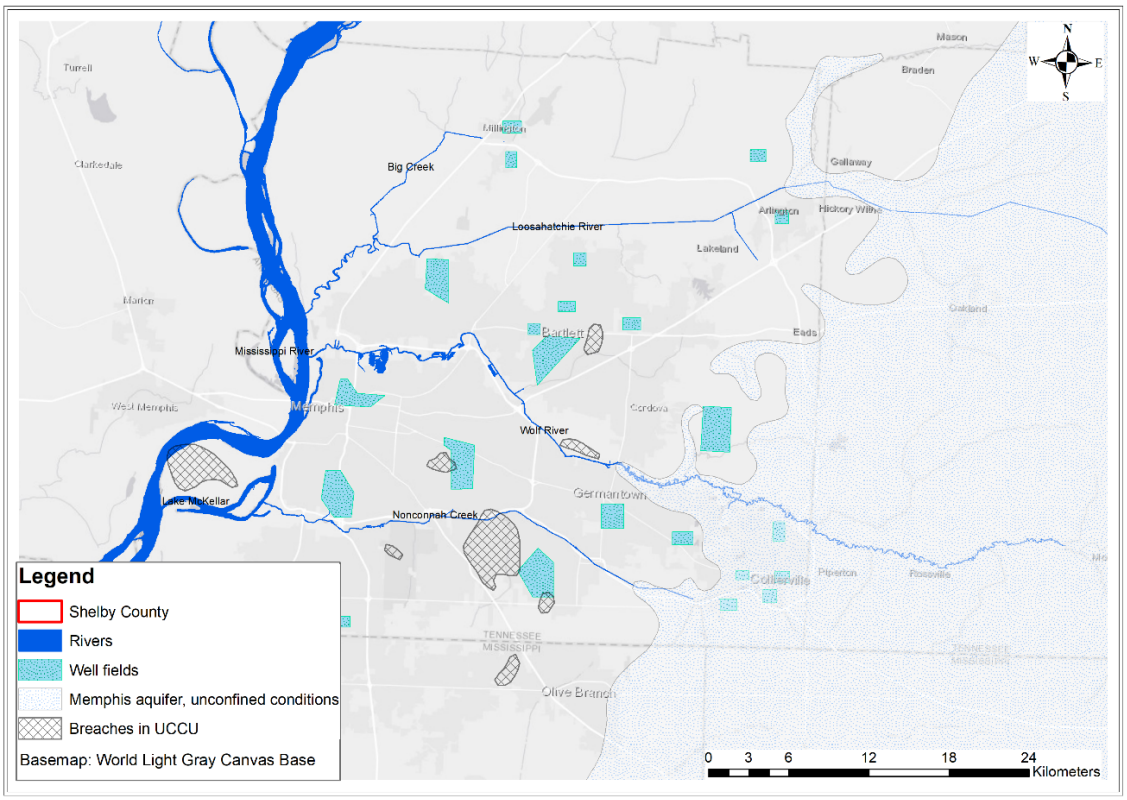

Figure 2. Map of the study area in Memphis (Shelby Co., Tennessee) highlighting rivers, wellfields, and showing breaches in the UCCU, and the unconfined zone of the Memphis aquifer as mapped by Parks (1990).

Depressions in the water table, as seen in water table maps of the unconfined aquifer, could correspond to probable breach locations, unless there are nearby high capacity production wells screened in the unconfined aquifer (Graham and Parks, 1986; Parks, 1990; Narsimha, 2007; Bradshaw, 2011; Gallo, 2015). Many such previous studies provide maps showing the probable location of the breaches. Most probably, previous studies do not provide enough information about all existing breaches in Shelby County, so that there are likely more breaches than those that have been mapped (Waldron *et al.*, 2009). There is a

need to locate these breaches for the sustainable management and protection of the Memphis aquifer including future land-use decisions, selection of sites for new well fields or landfills, and monitoring existing contaminated sites.

To locate breaches, it would be expensive and not very pragmatic to drill a large number of observation wells covering the whole county. Comparatively less expensive than drilling many exploratory holes, geophysical methods have been used in Shelby County to map breaches (Waldron *et al.*, 2009). However, a limiting factor for using these geophysical methods more throughout Shelby County is the density of urbanization that restricts access and produce significant background noise. It is thus necessary to develop additional methodologies to locate any unknown breaches and better characterize those that are already known or suspected. This research uses groundwater-surface water interactions to identify the potential location of breaches located in the proximity of the Wolf River.

During high flow conditions, streams contribute directly to an underlying unconfined aquifer (Brunke and Gonser, 1997). In contrast, groundwater is the primary source of river discharge in low flow conditions (Brunke and Gonser, 1997; Sophocleous, 2002). When the river stage is lower than the groundwater table, as is typical during the low-flow season, water will flow from the aquifer to the stream. However, the presence of a cone of depression in the water table near a stream could cause a decreased contribution from the aquifer or could even result in water flowing in the opposite direction, therefore, from stream to the aquifer (Brunke and Gonser, 1997; Sophocleous, 2002). For this reason, detecting reaches where a stream loses water during the low-flow period could help in identifying locations where the water table is locally depressed. In the case of Shelby County, cones in the water table should only occur either due to the presence of high capacity production wells or else to breaches that allow water to flow towards the deeper aquifer. Therefore, our research hypothesis is that locating losing reaches along a stream, under low-flow conditions, at

locations that are far from the influence of any pumping station, can help inform the probable location of nearby confining unit breaches.

The objectives of this research are:

1. To locate losing reaches along the Wolf River during low-flow condition at a coarse scale.
2. To investigate spatial patterns of vertical exchange flux to locate potential nearby breaches in the UCCU.
3. To compare the location(s) of any breach(es) located along the Wolf River with those described in the literature (Graham and Parks 1986; Parks 1990).
4. To better understand the variability of groundwater-surface water interactions over different spatial scales.
5. To compare different techniques (seepage meters, temperature sensors, piezometer, and differential stream gaging) for investigating groundwater-surface water interactions.

QUANTIFYING GROUNDWATER-SURFACE WATER INTERACTIONS

Historically, people considered groundwater (GW) and surface-water (SW) bodies to be different entities, and many GW-SW investigations were conducted assuming such condition. However, GW and SW bodies are hydrologically connected and act as a single resource (Winter *et al.*, 1998), so that changes in groundwater quantity and quality affect surface waters, and vice versa. Because the sustainability and protection of both types of water bodies requires understanding such reciprocal effects, the topic of GW-SW interactions is gaining much attention.

To successfully understand the interaction between GW and SW, one needs to quantify the direction and magnitude of the vertical exchange fluxes through streambeds.

However, such fluxes display a large temporal and spatial variability (Krause and Bronstert, 2007; Wang *et al.*, 2017), so that their characterization is challenging (Kalbus *et al.*, 2006). Various well-known techniques can be used for estimating the fluxes between groundwater and surface water, such as Darcy flux calculations, vertical temperature gradients, stream tracer experiments, differential stream gaging, seepage meters, and numerical modeling. Kalbus et al. (2006) stress that these have different resolutions, uncertainties, and limitations, so that the choice of an appropriate method depends entirely on the purpose of the investigation. Kalbus et al. (2006) and Rosenberry and LaBaugh (2008) discuss various field techniques to quantify GW-SW interactions, describing their advantages and issues.

For this research, seepage meters were initially used to get the general direction of the vertical exchange flux in the streambed, due to their simplicity and cost-effectiveness. Kalbus et al. (2006) suggest the use of multiple techniques at a single study area to give a better picture of the actual scenario. However, because it was not feasible to use multiple point-scale methods over the whole study reach, different techniques were compared only for those sub-reaches identified as losing in the preliminary screening. At the losing sub-reaches, piezometers were installed to calculate vertical hydraulic gradients and temperature sensors (iButtons) were deployed to measure temperature within the streambed, while simultaneously collecting data with seepage meters. Later, differential stream gaging was conducted to obtain integral assessments of stream discharge at the sub-reach scale, which were then compared to results from point-scale methods.

Seepage Meters

Seepage meters are a simple, direct, and cost-effective method to quantify GW-SW exchanges at the GW-SW interface (Rosenberry, 2008), and many studies of groundwater interaction with streams have been conducted with them (Lee and Hynes, 1978; Libelo and MacIntyre, 1994; Blanchfield and Ridgway, 1996; Cey *et al.*, 1998; Landon *et al.*, 2001). The

idea behind seepage meters was initially developed in the 1940s to quantify water loss from unlined irrigation canals (Israelsen and Reeve, 1944). Lee (1977) designed a seepage meter with a cylinder vented to a plastic bag and tested it in the laboratory. He observed a linear relationship between the measured seepage flux and an experimentally controlled hydraulic gradient. Lee's (1977) seepage meter can be used to measure the seepage flux in the bed of lakes and estuaries. Since then, seepage meters have been used in many studies to estimate vertical fluxes in beds of wetlands, lakes, ponds, estuaries, and oceans (Fellows and Brezonik, 1980; Lewis, 1987; Shaw and Prepas, 1990; Murdoch and Kelly, 2003).

Conventional seepage meters can give erroneous result when used in streambeds, due to the velocity head of the flowing water, seepage bag conductance, and effects caused by the geometry of the seepage bucket (Murdoch and Kelly, 2003). Rosenberry (2008) adjusted the traditional seepage meter design for application in running waters. He tested his device, concluding that seepage meters can still give erroneous values if not positioned correctly, due to current velocity. Thus, seepage meter measurements are less accurate in flowing water than in non-flowing conditions. Furthermore, they only provide a point-scale measurement, which can be difficult to upscale due to the large spatial variability of streambed properties (Calver, 2001; Kennedy *et al.*, 2010).

Differential Stream Gaging

Differential stream gaging is a widely used larger-scale technique to quantify net exchanges between groundwater and surface water (Cey *et al.*, 1998). The difference in discharge measured at two locations along the stream provides the net groundwater inflow or outflow, as long as contributions from surface runoff and tributaries are negligible between the points (McCallum *et al.*, 2012). According to McCallum et al. (2012), this method is feasible when the potential error in the discharge measurement is significantly lower than the discharge in the stream. Cey et al. (1998) used detailed streamflow measurements to estimate

vertical fluxes in the streambed during a baseflow period. They pointed out that even if the discharge is significantly higher than the error, it is difficult to quantify the net vertical flux over short distances, where the measured differences in streamflow will often be smaller than the error in measuring the flow.

One way of solving this issue is to adjust the distance so that the measured difference is higher than the error; another is to measure the discharge as accurately as possible, to minimize the error. The most reliable instrument to measure point velocities over a cross-section is the individually-calibrated mechanical current meter. Under wadable, low-flow and steady-state conditions, the accuracy of a discharge measurement performed with a current-meter depends on the performance of the instrument and the number and quality of observations of depth and velocity made at the given cross-section (Carter and Anderson, 1963). According to Carter and Anderson (1963), all errors, except instrumental ones, can be reduced by increasing the number of observation points in the section, but it is difficult to justify the added costs. Discharge is computed using the velocity-area method, as a linear sum of flow velocity over the channel cross-section (Le Coz *et al.*, 2012).

Mini Piezometers

Mini-piezometers are easy-to-construct, cost-effective, small-dimension observation wells, often used to measure the vertical hydraulic gradient between groundwater and a surface-water body such as a stream or lake. The observed groundwater piezometric head from the mini-piezometer is compared with the surface-water level to obtain direction and hydraulic gradient of water flow near the GW-SW interface. There are various types of piezometers made with a solid pipe or flexible tube, but all are functionally the same. The choice of material depends on the situation in the field, the scale of the measurement, and cost aspects.

The main drawback of using mini-piezometers relates to the inherent difficulties in measuring a small hydraulic head difference. Thus, mini-piezometers are often combined with manometers to increase measuring accuracy (Lee and Cherry, 1979; Winter *et al.*, 1988; Baxter *et al.*, 2003) but it can still be difficult to resolve the minute hydraulic head differences that often occur in fine streambeds (Kennedy *et al.*, 2007). In addition, the manometer adds more complications and problems due to leaks between connections and gas bubbles from groundwater (Kennedy *et al.*, 2007). Kennedy et al. (2007) designed mini-piezometers with an oil-water manometer to solve some of the issues with conventional manometers, but these are expensive to use on a large scale.

Temperature Sensors

When water is exchanged between ground and surface waters, there is also a flux of heat between these water bodies (Bouyoucos, 1915). Many studies (Silliman and Booth, 1993; Silliman et al., 1995; Anderson, 2005; Constantz and Stonestrom, 2003) have used heat as a tracer for estimating GW-SW exchange. Usually, the groundwater temperature does not fluctuate much but the surface water temperature has both diel and seasonal cycles. Measuring temperature at different depths, in order to obtain the vertical temperature profile in the streambed, can give an indication of the nature of the flux (Becker *et al.*, 2004; Essaid *et al.*, 2008). In a gaining stream, the temperature profile of the streambed is more influenced by the temperature of the groundwater, whereas in a losing stream, the temperature along the profile will be more similar to that of surface water (Essaid *et al.*, 2008) as shown in Figure 3. Hence, one should expect that the temperature at depth fluctuates less in gaining conditions, and more in losing conditions. In this research, temperature sensors (iButtons) were used to measure the temperature at different depths in the streambed, in order to identify the direction of the vertical streambed flux.

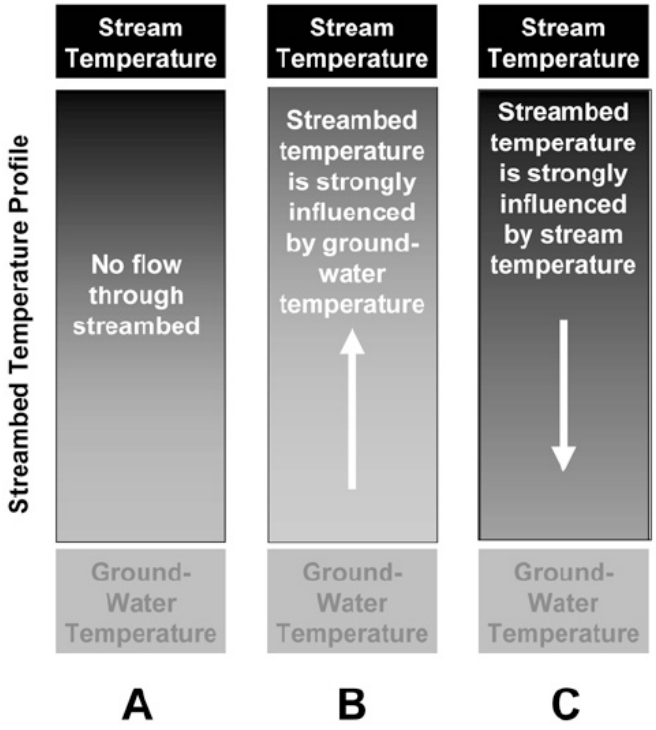

Figure 3. Expected streambed temperature profile for (A) a neutral stream, (B) a gaining stream, and (C) a losing stream (Source: Essaid *et al.* 2008)

SITE DESCRIPTION

Our study reach covers 49 km of the lower Wolf River, which is a tributary of the Mississippi River that flows westward through Shelby County, Tennessee. The spring-fed Wolf River has its headwater in Holly Springs National Forest, Mississippi, and is 169 km long. The 2110 km^2 watershed of the Wolf River lies in west Tennessee with a sizeable portion in north Mississippi (Figure 4). The channel of the Wolf River consists of loose unconsolidated alluvium, whereas its flood plain is composed of Holocene, saturated, unconsolidated sand overlain by clayey silt (Broughton *et al.*, 2001). The Wolf River watershed is within a humid-temperate climate, with a rainy season occurring from October to March and a dry season from April to September.

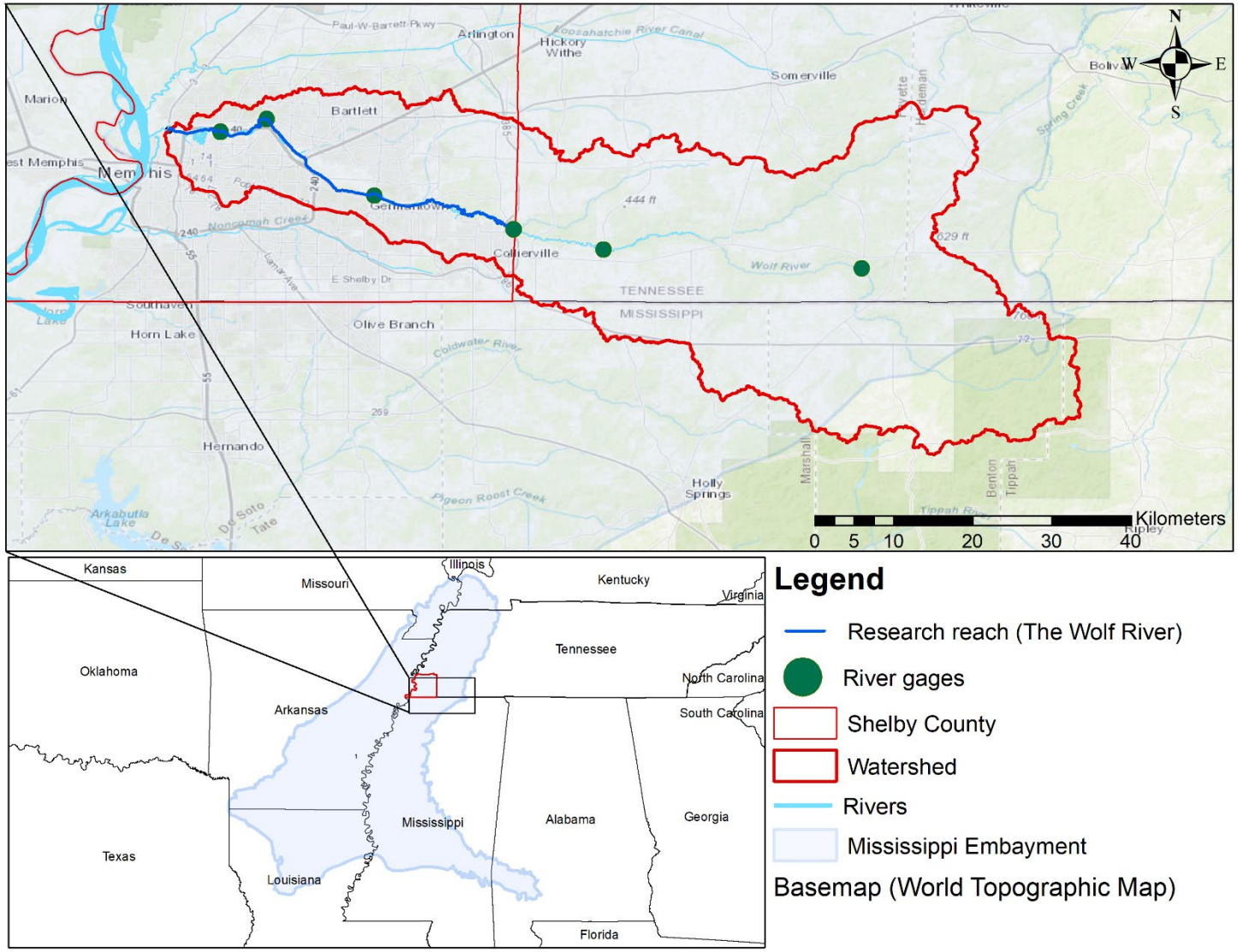

Figure 4. Map of the study area in Shelby Co., Tennessee, highlighting the research reach on the Wolf River, and depicting its watershed and the Mississippi Embayment.

The 50 years of daily discharge records at gage "USGS 07031650 Wolf River at Germantown, TN," located at the Germantown Parkway bridge, show a typical low-flow season discharge of around 6 m^3/s, while the highest peak flow recorded was 946 m^3/s. The Wolf River stage changes dramatically during and immediately following rainfall event, as shown in Figure 5. The data were collected during the dry season (July 2019 to October 2019). The minimum stage was 0.83 m, whereas the maximum reached a value of 5.10 m.

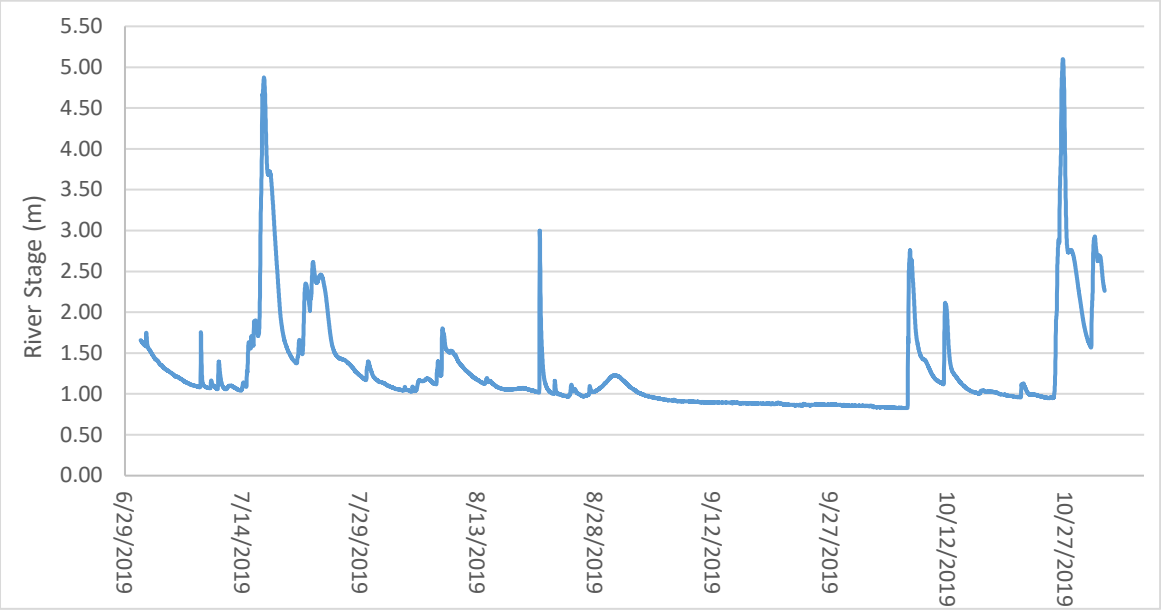

Figure 5. Stage height at gage "USGS 07031650 Wolf River at Germantown, TN" (July 2019 to October 2019) during the study period

Since 1964, the lowest 35.4 km of the Wolf River have been channelized to decrease flooding, and the floodplain breadth has been reduced by about 50% due to filling and land development (Van Arsdale *et al.,* 2003; Yates *et al.,* 2003). These changes in the dimension of the channel and floodplain have increased the water velocity, cross-sectional area, and conveyance capacity (Van Arsdale *et al.*, 2003). Yates et al. (2003) mention that the entrenchment of the Wolf River and its flood plain may have enhanced the connectivity between Wolf River surface water and the underlying aquifer, which increases the potential for its contamination.

APPROACH AND METHODS

This study of GW-SW interactions to identify breach locations comprised three phases. As the first phase was expected to cover the full 49 km reach of the Wolf River within Shelby County, we focused on a cost- and time-effective methodology. Further resources then went into the more robust methods (Ott current meters and drilling) used in the second and third phases, at finer scales. The first phase sampled the full 49 km reach along the lower Wolf River using cost-effective seepage meters at a spacing of 100 m. Its results offered a better idea of those sub-reaches where the Wolf River could potentially be losing water. In the second phase, losing areas identified in the first phase were examined at a finer scale using multiple techniques such as seepage meters, piezometers, temperature sensors and differential stream gaging. In the final third phase, water levels of the Wolf River, the unconfined aquifer, and the confined Memphis aquifer in those losing areas were monitored to confirm the potential presence of a breach nearby.

First Phase: Full Reach Scale

Identifying the best method for investigating GW-SW interactions along a 49 km-long river reach is challenging. Seepage meters and piezometers were chosen as the best candidates for this first phase, due to their simplicity, directness, cost-effectiveness, and the fact that they are easier to construct and deploy in the field. However, seepage meters measure the cumulative flux of water over a sampling duration, which makes it easier to infer losing or gaining conditions, as compared with piezometers. The expected head differences are very small in sand-bed streams such as the Wolf River, so it can be challenging to discriminate them from the velocity-head effects around the pipe. This was the case in a previous local study by Pickett (2012), who found that head differences were so minute that a laser with 0.1 mm accuracy was required to measure them. For this reason, seepage meters

were selected for the study's first phase, in an attempt to obtain a broader scale evaluation of losing segments along the Wolf River.

Seepage meters measure vertical exchange fluxes near the GW-SW interface (Rosenberry, 2008). The direction and magnitude of the vertical exchange flux at the riverbed are obtained by comparing the amount (weight) of water gained or lost by the seepage bag between the times of deployment and pickup. A positive difference (seepage bag gains weight) reflects a gaining condition, whereas a negative difference (seepage bag loses weight) indicates a losing condition.

Design. The cost-effective seepage meter design included a seepage bucket, a seepage bag (catheter bag) with a valve, and a housing or shelter for the bag (Figure 6). A 5-gallon bottom-cut bucket was used as a seepage bucket; its top was sealed with a lid, while the bottom remained open. The lid had a hole with a tightly closing rubber seal to facilitate passage of the seepage bag tube, which in turn lead to a 2000 ml catheter bag. The tip of the catheter bag tube was fitted with a barb-ball valve to start or close the flow. The catheter bag was initially filled with a known starting mass (about 1000 g) of water, to eliminate any anomalous initial gain while connecting the catheter bag to the seepage bucket (Shaw and Prepas, 1989; Blanchfield and Ridgway, 1996; Rosenberry, 2008). The catheter bags were checked for any possible leak by comparing their weights before and after a 12-hour interval, and any identified punctures were fully sealed. Another 5-gallon bucket was used as a shelter for the seepage bag; it contained a few holes so that water could freely enter or leave, without changes in pressure, in response to the changing volume of the bag. This shelter was used to eliminate velocity impacts of the stream on the bag (Rosenberry, 2008). A total of 90 seepage meters were constructed for this study.

General Seepage Meter Installation Process. First, the open-bottom seepage bucket was pushed about 10 in (25 cm) into the riverbed, ensuring that there was no air trapped

inside. Care was taken to ensure a good seal between bucket and lid, and bucket and sediment. Some riverbed material was placed inside the shelter bucket, so that it could not get dislodged by the impinging flow, and it was then placed in the lee of the seepage bucket. The catheter bag was placed inside the shelter bucket, and its lid was closed so that the bag could not float away. The shelter bucket was placed immediately downstream of the seepage bucket. Then, the green tip of the catheter bag tube was connected to the seepage bucket through the rubber seal in its lid, and the valve was opened. The seepage bag was sampling from that moment on.

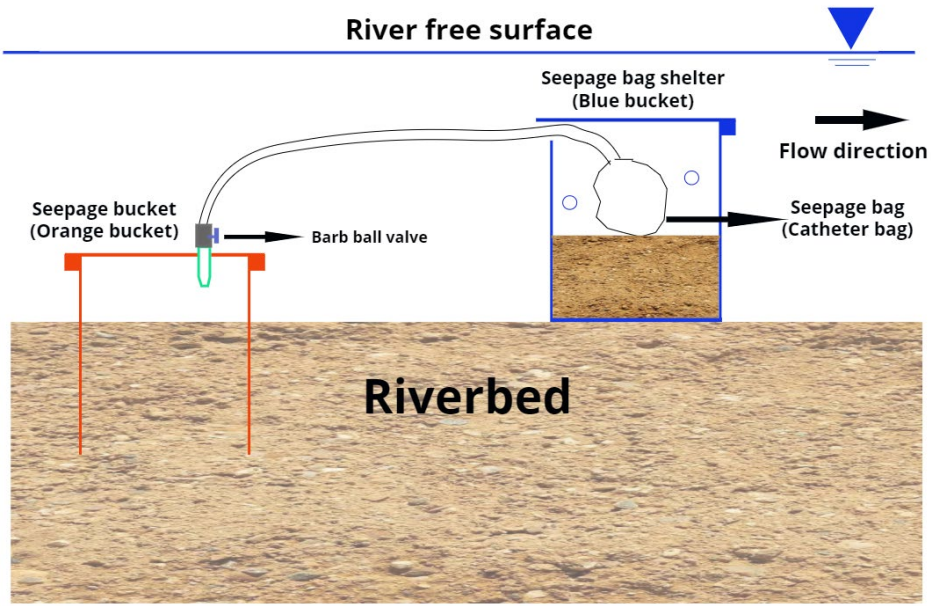

Figure 6. Seepage meter design and installation.

Data Collection. All known access points to the Wolf River were identified during preliminarily and field visits were performed to collect information about their condition for safe and easy access. Considering all available access points as well as number of deployment sites, the full 49 km-long reach of the Wolf River within Shelby County was mapped and divided into a series of sub-reaches, each with defined entry and exit points, so that each one could be covered in one day. The seepage meter deployment was performed

using three teams – reconnaissance team, deployment team, and pick-up team - with two canoes per team.

Before deployment, all individualized catheter bags were filled with an initial weight of water (about 1000 g) and their valve was closed, ensuring there was no air trapped inside the bag or its tube. The first, "recon" team, located each deployment point (at 100 m spacing) using ESRI's collector mobile app which was preloaded with the coordinates of each point. They installed pre-flagged, and pre-taped bamboo poles as visual markers, and then recorded the geomorphic setting, such as type of riverbed material, river morphology, water depth, etc., of the river at each position. The deployment team started floating downriver after the recon team, carrying the pre-filled and pre-weighed catheter bags, seepage buckets, shelter buckets, and all required equipment. No farther than a few feet from each flagged bamboo pole, they installed a seepage meter at a location where the flow depth was sufficient to fully submerge all of its parts, recording installation time, bag number, and location number. The pick-up team started floating down one hour after deployment, to allow for the seepage measurement time to be at least one hour. Before checking the status of the seepage meter, the valve was closed, then the team removed everything from the deployment location, documenting the time of recovery, the bag number, and the location number in their observation sheet.

Once on land, all recovered bags were immediately weighed. The difference in water content before and after the installation was then used to calculate the gain or loss at each location, which was mapped in ArcGIS. It took 12 full days of fieldwork to complete the first phase of this research.

Second Phase: Sub-Reach Scale

After conducting the first phase, gain or loss were mapped at every 100 m, along the full 49 km of the lower Wolf River. The map was compared and analyzed in light of available

information from the literature (Parks 1990; Narsimha 2007; Ogletree 2016). Sample statistics were computed, and the gain/loss data were plotted on maps to check for any obvious spatial patterns. In order to account for the possible influence of background overall gaining conditions along the reach, which would result in a prevalence of gaining points, the data were also replotted after splitting the sample in "larger gain" and "lower gain and loss" groups, using different thresholds (e.g., 2 g/min, 5 g/min, 8 g/min, etc.).

Because the presence of breaches should affect the gain/loss patterns at a relatively large spatial scale, a series of analyses were performed using ArcGIS for Desktop to try to understand the spatial structure of the seepage meter data. First, the "Spatial Autocorrelation (Global Moran's I)" tool was used to check for randomness or the possible presence of clusters. This tool measures spatial autocorrelation for a variable along a line, based on its location and value simultaneously, by calculating a z-score, which is a measure of the intensity of clustering. Having found strong clustering in the seepage meter data, the "Incremental Spatial Autocorrelation" tool was then used to obtain a typical reach length at which the clustering is most significant. This tool measures the intensity of spatial clustering by calculating the z-score for a series of increasing distances. The z-score usually increases with increasing distance, peaking at some particular value (or multiple values), which corresponds to that length scale at which the spatial process promoting clustering is most noticeable. This resulting length was selected as the threshold distance to subsequently perform hotspot analysis, to detect spatial patterns in the data. The ArcGIS hotspot analysis tool compares each value with its neighboring values within the given threshold distance, identifying hotspot areas where high values are surrounded by other high values, and cold areas where low values are surrounded by other low values.

These analyses helped identify the location of potential losing sub-reaches along the Wolf River, for further investigation at a finer scale. For the second phase of data collection,

three such locations were identified and investigated, using multiple point-scale methods as well as a reach-scale, integrative method to better understand the spatial variability of GW-SW interactions over a range of scales.

Point-Scale Methods. Multiple point-scale methods such as seepage meters, piezometers, and temperature sensors (iButtons) were applied over closely spaced grids covering sub-reaches of about 600 m in length, as shown in Figure 7. In addition to indicating the direction of the vertical flux, the seepage meters give a cumulative measurement of gain or loss over time, whereas piezometers readings allow computation of the vertical hydraulic gradients between different depths. Recording temperature at different depths provides a vertical temperature profile in the streambed that should indicate the direction of the vertical exchange flux, as surface water is warmer than groundwater in summer. This approach enables comparison of data obtained with three different point-scale methods, minimizing the limitations of using any single, specific method; thereby, allowing better understanding of the spatial variability of vertical streambed fluxes at the smaller scale.

Each grid had three or five rows (Figure 7), depending on location. A 50-m spacing was chosen between the grid columns, adding additional measurement transects around the point where results from the first phase indicated losing conditions, to investigate the sub-reach at a finer spatial scale. The size of the grid and the number of grid points were selected in a way that data collection at each one of the three sub-reaches could be completed in one day, to avoid possible temporal variations in the measurements. Spatial autocorrelation analyses were performed on the seepage rates obtained at this finer scale, to better understand and describe the spatial structure of the data.

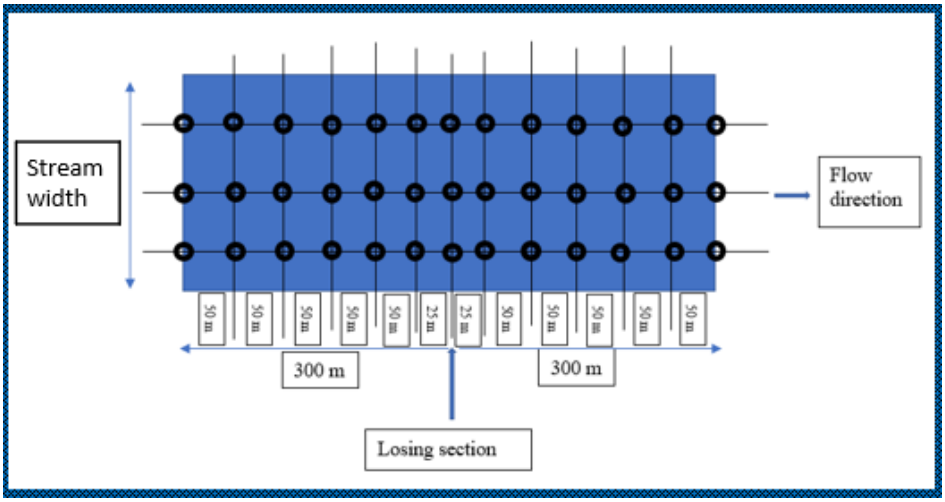

Figure 7. Typical grid setup used at the finer scale, in this case with three rows, to apply multiple methods

Vertical Hydraulic Gradient. To compute the vertical hydraulic gradient, mini-piezometers were constructed using 1.5 m-long, 1.9 cm (0.75") diameter, Schedule 40 PVC pipe. Multiple holes were drilled in the bottom 10 cm of the pipe, as a screen, which was then wrapped with filter (screen) fabric to prevent clogging by fine sediment. A driving point was glued to the bottom of the pipe to facilitate inserting it into the sediment. The pipe was marked every 10 cm from the middle of the screen, to facilitate installation of the piezometers at the required depths.

The groundwater piezometric head, i.e., the water level inside the mini-piezometer, and the surface water head (water level outside the mini piezometer), were measured using a metric steel tape. The backside of the tape was roughened, so that chalk could stick to it. Before each single measurement, the tape was dried and cleaned, before applying colored chalk. This allowed us to measure the depth of water from the top of the piezometer. It was challenging to measure the surface water head outside the piezometer, due to the fluctuating effect of velocity head on the outer surface of the pipe. A hollow bucket was placed around the pipe in an attempt at reducing the disturbance, so that we could accurately measure the depth to the surface water with the steel tape. After driving each mini-piezometer, we

provided at least 20 minutes of stabilization time before measuring outside and inside depths. The vertical hydraulic gradient was then computed as the difference in measured depths divided by distance from the streambed surface to the depth of the middle of the screen.

Vertical Temperature Profile. All iButtons were programmed before going to the field so they would measure temperature every 1 minute. Temperature data were collected at two of the sub-reaches, using slightly different approaches. In the first, the same mini piezometers used to measure piezometric heads housed an iButton centered at the mid-depth of the piezometer screen, which logged temperature (see Figure 8). The piezometer screen was first driven to a depth of about 30 cm below the riverbed. After allowing 20 minutes of stabilization time, it was further driven to a depth of 80 cm, allowing for 40 minutes of stabilization time before removing it. During this time, the iButton recorded the temperature within the streambed at 30 cm depth (for 20 minutes) and at 80 cm depth (for another 40 minutes). The temperature readings logged just before pushing to further depth and just before retrieving the piezometer were taken as the instantaneous temperatures at depths of 30 cm and 80 cm from the streambed, respectively.

In the second approach, we used a 1.9 cm (0.75") diameter, Schedule 40 PVC pipe equipped with four iButtons to simultaneously measure water temperature under the streambed at different depths. A piece of pipe was divided into three disconnected, 40 cm-long compartments. At the bottom 10 cm of each compartment, holes were drilled to form a screen which was wrapped with filter fabric to prevent clogging, and an iButton was then placed in the compartment. A fourth iButton was placed outside of the pipe, further up, to measure the water column temperature. The pipe was driven into the streambed, with iButtons logging at depths of 20 cm, 60 cm, and 100 cm below the streambed, as shown in Figure 8 (right). The pipe assembly was left for 25 minutes at each sampled location. The

values logged just before retrieving were taken as the temperature at each given depth, and for the surface water.

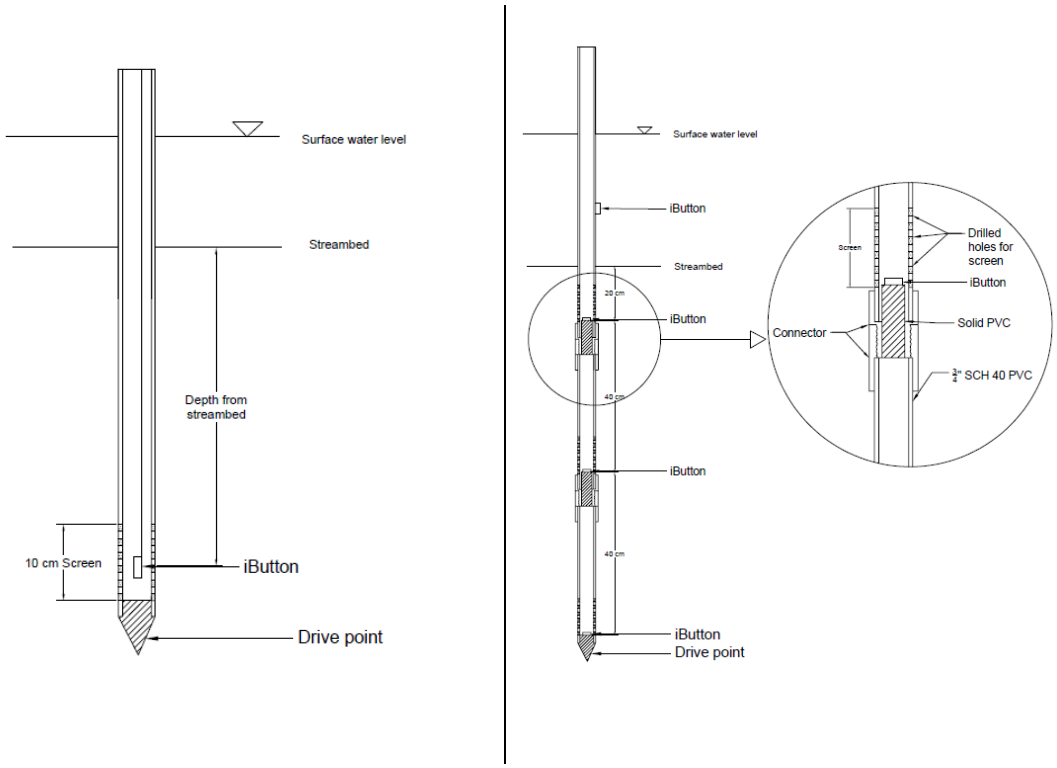

Figure 8. Two slightly different approaches used to measure the instantaneous temperature profile

The average water temperature of the unconfined aquifer in Shelby County during the low-flow period (summer) is about 18-20 °C, while that of surface water is about 25 °C, fluctuating along a diel cycle (U.S. Geological Survey, National Water Information System: mapper. Accessed August, 2020, https://maps.waterdata.usgs.gov/mapper.). At gaining locations, we would expect to observe a difference in temperature between the shallow and the deeper measurements, as shown in Figure 3, with no diel fluctuation in temperatures at depths due to surface water effects. Conversely, at losing locations the difference in temperatures between different depths should be very small, and the diel fluctuations in surface water temperature should propagate deeper into the streambed.

Differential Stream Gaging at Reach-Scale. To estimate whether our study reaches are losing or gaining and to corroborate the results obtained at the point-scale, differential

stream gaging was conducted during low-flow, near steady-state conditions. We used Ott C2 current meters with individually-calibrated propellers (see Figure 9); these are highly precise small current meters for discharge measurement in small rivers, with an accuracy of ±1%.

Figure 9. Ott C2 current meter body, rod, and propeller

For this study, each measurement cross-section was divided into approximately 40 verticals, choosing these with the intention that discharge between any two verticals be less than 5% of the total discharge (EN ISO 748:2007). The six-point method was used to calculate average velocity over each vertical. The depth at each vertical and at the midpoint between two verticals (termed bathymetric verticals hereafter) were measured to obtain the cross-section profile (Figure 10). The velocity at each of the six points per vertical was calculated using the individually-calibrated equation provided for each combination of current-meter body and propeller. Each point velocity was obtained as an average over a 60-second sampling time. To shorten gaging times, we took simultaneous readings at three depths by mounting three current meters on the same rod. Then, the average velocity at each vertical was calculated using the six-point equation provided by EN ISO 748:2007:

$$V = 0.1 * \left(v_{surface} + 2 * v_{0.2} + 2 * v_{0.4} + 2 * v_{0.6} + 2 * v_{0.8} + v_{bed} \right) \quad (1)$$

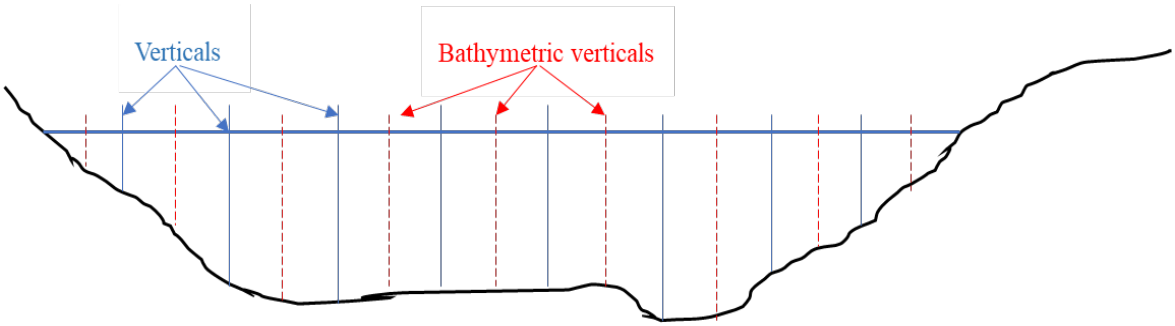

Figure 10. Additional bathymetric verticals between the velocity measurement verticals

To better estimate the total discharge, velocities at the bathymetric verticals (Fulford and Sauer, 1986) were estimated using an interpolation based on the Froude number (see Figure 11) as proposed by several references (Fulford and Sauer, 1986; Boiten and IHE Hydrometry, 2000; Le Coz *et al.*, 2012, 2014).

The Froude number was calculated at conventional (measured) verticals using the equation:

$$Fr_{i-1} = \frac{V_{i-1}}{\sqrt{g * h_{i-1}}} \tag{2}$$

While the Froude number at each bathymetric vertical was then estimated by interpolation:

$$Fr_i = \frac{[(x_{i+1} - x_i).Fr_{i-1} + (x_i - x_{i-1}).Fr_{i+1}]}{x_{i+1} - x_{i-1}} \tag{3}$$

Finally, the average velocity at bathymetric verticals was then computed as:

$$V_i = Fr_i . \sqrt{g * h_i} \tag{4}$$

In this fashion, the vertically-averaged velocity were calculated in both conventional (measured) and bathymetric (estimated) verticals. With these, total discharge at the cross-section was calculated using the velocity-area method.

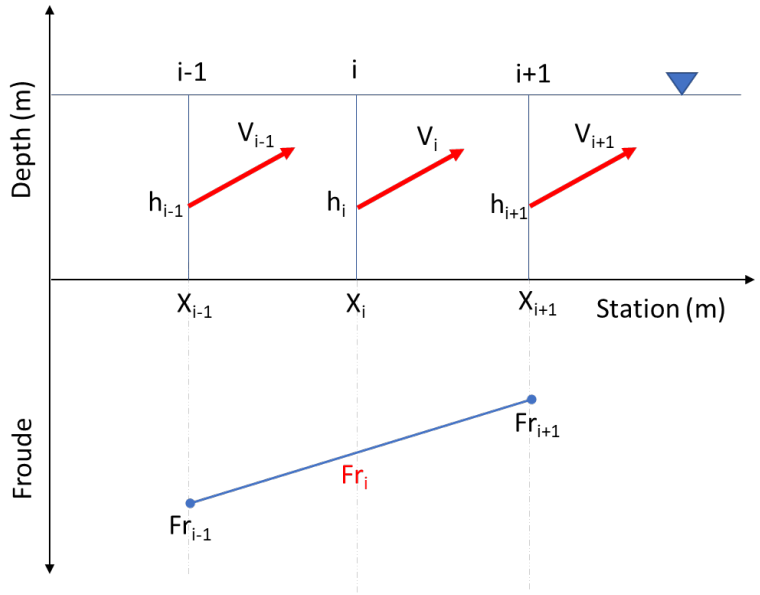

Figure 11. Average velocity associated with bathymetric vertical (v_i) by interpolation of the Froude number from adjacent verticals along a cross-section.

The discharge measurements at the two cross-sections were performed over the same time window by two different teams using the same techniques and equipment, so that any minor change in discharge during the gaging periods should have affected both sections equally. The discharge values obtained at two cross-sections were compared to each other to determine whether there is a significant net difference, considering their uncertainty. A significantly lower discharge at the downstream section indicates that the reach is losing water, whereas a higher discharge at the downstream section indicates the opposite. The uncertainty in discharge measurements were calculated using EN ISO 748:2007. For this determination, at 95% confidence level the calculated expanded uncertainty (two standard deviations) is 3%, considering a standard normal distribution. The overlapping area (see Figure 12) between two normal distributions (probability density functions) was computed as a way to check whether the discharges at the two cross-sections are significantly different.

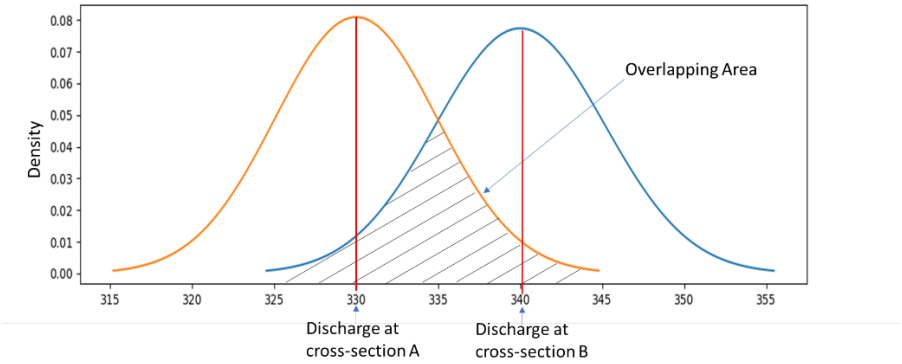

Figure 12: Typical comparison of two normal distributions centered about the gaged discharges at two cross-sections A and B, showing the overlapping area between them.

Third Phase: Monitoring River Stage and Groundwater Levels

Based on the results of the first and second phases, continuous monitoring of the changes in river stage and head in the unconfined aquifer water table and underlying confined aquifer was examined at one specific reach near Lansdowne Park in Germantown. A stilling well in the river and two monitoring wells – one screened in the unconfined aquifer and the other in the confined aquifer – were installed close to each other in the riparian zone. Solinst Levelogger transducers were installed in each well to continuously record absolute pressure and water temperature every 15 minutes, whereas a Solinst Barologger was installed to log atmospheric pressure. Water stages were calculated by barometric compensation of the absolute pressures obtained from the transducers. The dynamics of the river stage were then compared with the levels of the water table of the unconfined aquifer and the potentiometric levels of the confined aquifer to investigate the connection between the river and neighboring aquifers.

RESULTS AND DISCUSSION

First Phase: Full Reach Scale

Originally, the first phase of seepage meter deployment included 489 locations along the Wolf River, of which 89 were found to be unsuitable because water was either too deep or access was unsafe. Seepage bags were weighed in the field immediately before and after deployment. The difference in weight was computed over the deployment duration, known as the "seepage weight". A positive seepage difference (before – after) in weight indicates gaining, while a negative difference reflects losing conditions. Seepage rates (g/min) were calculated for each location by dividing the seepage weight (gram) by the total time of deployment (minute). These results are summarized in Table 1 and shown in Figure 13. It should be noted that in the case of positive values, the term "higher seepage rate" refers to a location where the river gains water at a higher rate, while "lower seepage rate" indicates a smaller flux, but still under gaining conditions.

Table 1: Statistics of seepage rates obtained from installing seepage meters every 100 m along a 49 km reach of the Wolf River

Total data points	Minimum Rate (g/min)	Mean Rate (g/min)	Median Rate (g/min)	Maximum Rate (g/min)	Standard Deviation (g/min)	No. of losing points	No of gaining points
400	-6.2	11.4	10.2	30.0	9.0	14	386

The statistics in Table 1 indicate that there is a huge range of variation in seepage rates, suggesting high spatial variability in the vertical exchange fluxes at this scale. This spatial variation is due to the heterogeneity of the hydraulic conductivity of the streambed material, the differences in vertical hydraulic gradients, possible effects of hyporheic exchange, and errors related to measurement instrument and application techniques. The data show that most sampled points along the Wolf River are gaining water, which should be expected in Shelby County during a low-flow period (Villalpando-Vizcaíno 2019).

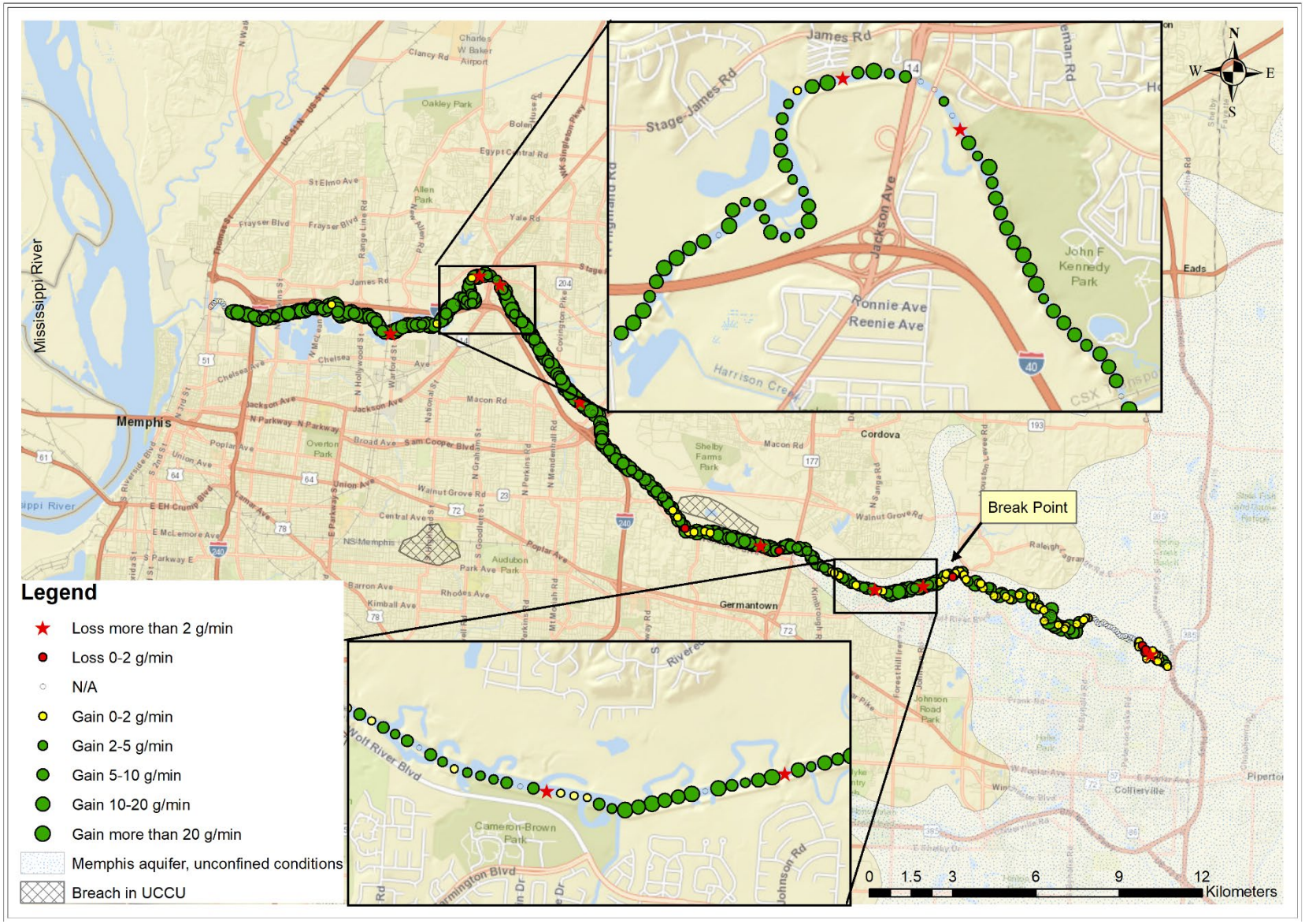

Figure 13. Calculated seepage rate and direction for seepage meter measurements (100 m spacing) conducted in the lower 49 km reach of the Wolf River within Shelby County, Tennessee. Two areas have been enlarged to clearly show the rates and direction.

It is important to mention that the full 49 km reach includes two very different sub-reaches, in terms of channel type. The upper 14 km of the reach, above the break point shown in Figure 13, are meandering, whereas the lower 35 km are channelized. The average seepage rate for the first 14 km reach is 4.7 g/min, whereas it is 13.2 g/min for the channelized reach, a significantly different value according to a t test (p value < 0.0001). This higher seepage rate in the lower reach might be due to augmented connectivity between the Wolf River and the underlying aquifer after the channelization process, as suggested by Yates et al. (2003). The lower seepage rates in the meandering reach might also be related to the occurrence of hyporheic exchange flow, which is enhanced at bends (Winter et al. 1998). Also, the upper 14 km reach lies within the unconfined portion of the Memphis aquifer (Parks, 1990), where one should expect losing conditions, or at least lower seepage (gaining) rates.

The map (Figure 13) shows that only 14 of the 400 measured points are in a losing condition. In most cases, the losing points are not clustered but are separated by several gaining points. At first glance, looking only at losing versus gaining conditions, there is no obvious pattern suggesting predominantly losing areas. This could be simply due to the fact that our measurements do not allow us to discriminate losing patterns if an expected depression in the shallow water table, as related to a possible breach in the confining layer, is not substantive. The single area along the study reach where previous studies strongly suggest the presence of a breach (Graham and Parks, 1986; Parks, 1990; Gentry *et al.*, 2006; Waldron *et al.*, 2009; Schoefernacker, 2018) and a downstream decrease in the discharge was documented (Bradley, 1991), near a Closed landfill in Shelby Farms Park, does not conclusively reflect a losing pattern; however, it does contain a single losing point.

There is an underlying issue related to a mismatch in scale between what we are trying to detect and the observation scale of the measurement method. Seepage meters integrate over a spatial scale the size of a 5-gallon bucket (30.2 cm diameter), and there could

be a range of factors, e.g., hyporheic exchange fluxes, that could inordinately influence the measurement. Basically, it is possible that this small-scale noise is not allowing us to detect overall patterns of losing/gaining conditions.

In the simplified model mentioned in the introduction, the presence of a breach in the periphery of the river is assumed to result in losing conditions under low-flow conditions. But it might well be the case that the presence of a breach only affects the overall GW-SW flow patterns, without causing extensive losing conditions. In such a case, one may still observe gaining conditions overall, but seepage rates would be smaller than those found at locations without a breach. To analyze this possibility, the data was scrutinized in relative terms by splitting the sample in "larger gain" and "lower gain or loss" groups, according to different threshold values, before plotting. A clear spatial pattern appeared for seepage rates below threshold values of 2 g/min, 5 g/min, and 8 g/min. This spatial clustering, as observed for a threshold of 5 g/min, is shown in Figure 14-I.

In general, movement of water at the GW-SW interface (or hyporheic zone) occurs mainly due to GW-SW interactions and local hyporheic exchange (Woessner, 2000). Because of this, there is a need to use methods that are able to separate those two effects, as GW-SW interactions at the larger scale are of specific interest. Local hyporheic exchange occurs at relatively small spatial scales, whereas GW-SW interactions are larger-scale phenomena, as explained by Boano et al. (2014). Boano et al. (2014) showed how hyporheic flow occurs at scales ranging from centimeters to tens of meters governed by channel landforms such as submerged bedforms, bars, cascades, riffles, and meanders. The vertical motion of water due to hyporheic exchange is most likely random at a larger scale, such as our study reach. On the other hand, the overall movement due to GW-SW interactions depends on the level of the water table with respect to river stage, which is a phenomenon at a much larger spatial scale, so that it should be reflected at the reach scale. To check for spatial patterns at this large scale

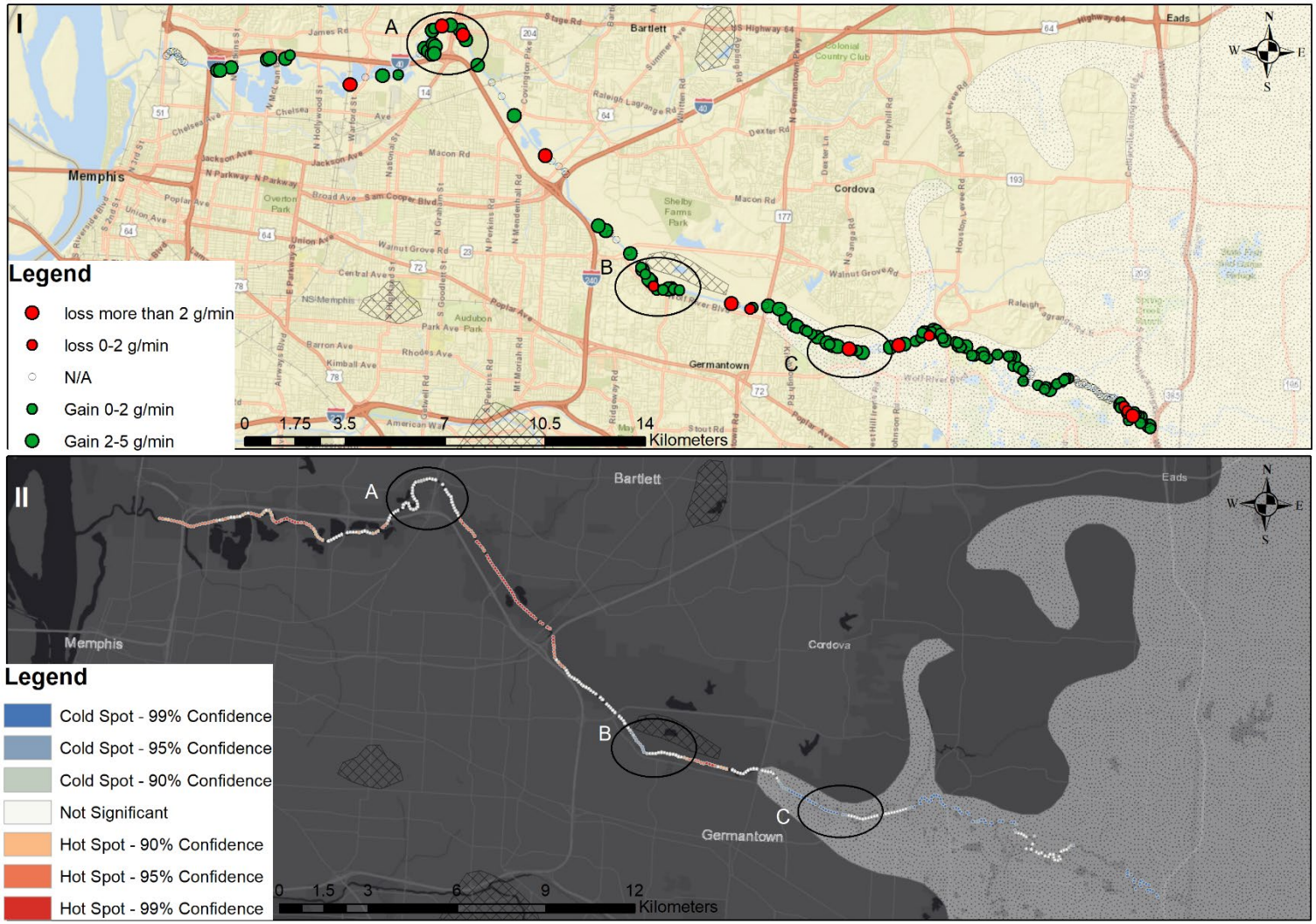

Figure 14. Map of the lower 49 km reach of the Wolf River showing locations with seepage rates below a threshold value of 5 g/min (I) and results from ArcGIS "Hotspot Analysis" tool (II), highlighting areas of interest A, B, and C.

we conducted a randomness analysis with the data, using the “spatial auto-correlation” tool in ArcGIS. This calculates a z-score, which is a measure of the intensity of spatial clustering. The results of this analysis are presented in Figure 15 The p-value of less than 0.01 (for z-score of 8.34) shows that the seepage rates are significantly clustered.

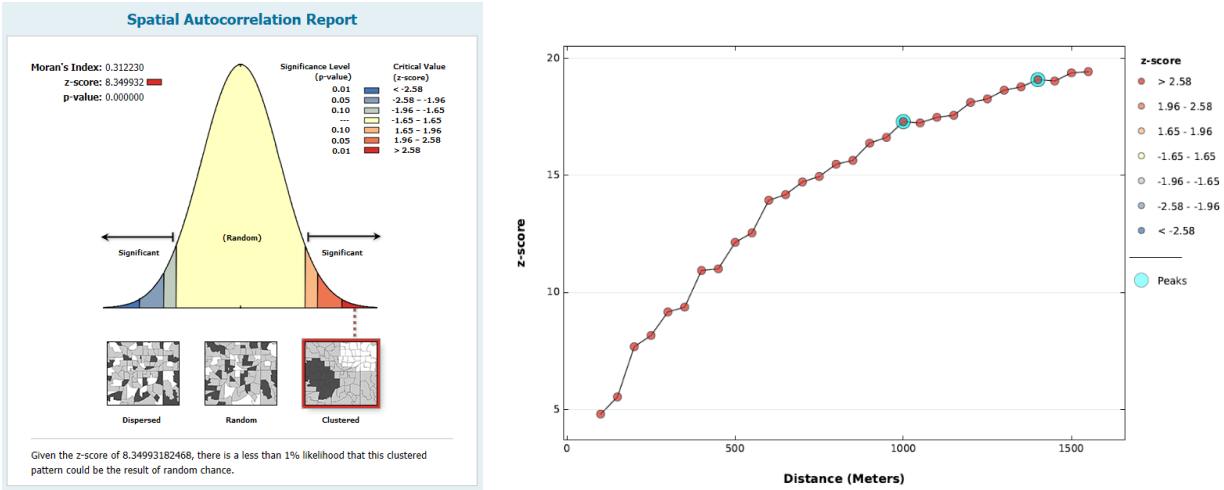

Figure 15. Results from using the “spatial auto-correlation” tool (left) and “incremental spatial correlation” tool (right) in ArcGIS with seepage rates at 100 m spacing along a 49 km reach of the Wolf River.

The “Incremental spatial correlation” tool was then used with an increment of 50 m to find that distance at which clustering is most profound. The result (Figure 15-right) shows that clustering is slightly more significant at 1000 m (first peak). Physically, the distance over which clustering is more pronounced should also represent the spatial extent of depressions in the shallow water table, caused by a breach. The influence of a breach on the water table depends on its properties; however, the properties of the breaches and their impact to the water table are not fully known. The shallow groundwater maps provided by Narsimha (2007) and Ogletree (2016) show that the radius of the water table depression near a known breach area (closed landfill, Shelby Farms Park) is approximately 1000 to 1500 m. Based on existing water table maps and the incremental spatial correlation analyses, a distance of 1000 m was then assumed as that length scale at which spatial clustering should be significant, and subsequently used to map clusters with hotspot analysis in ArcGIS. The result is shown in

Figure 14-II, where hot spots are the area where higher seepage values are surrounded by other larger values as well, while cold spots are those areas where lower values are surrounded by other low values. It is important to mention that the cold spots are those areas where the Wolf River is gaining less water, in relative terms.

Comparing this latter result with the original "threshold" map, as shown in Figure 14, similar spatial patterns are observed. Cold spots contain clusters of points with seepage rates below a given threshold value. Three sub-reaches: A, B, and C as shown in Figure 14, were chosen as close to potential breach locations for further, detailed study, based on the aforementioned analyses and site accessibility.

Second Phase: Sub-Reach Scale

Seepage Meters Deployment over a Closely Spaced Grid and Differential Stream Gaging

Area Downstream of Austin Peay Highway (Sub-reach A). Seepage meter data were collected on September 20, 2019. The mean river discharge and stage on that day were 7.76 m^3/s and 0.88 m, respectively, at the "USGS 07031650 Wolf River at Germantown, TN" gage (located 16 km upstream), while they were 8.5 m^3/s and 4.08 m, respectively, at the "USGS 07031740 Wolf River at Hollywood St at Memphis, TN**"** gage (located 6 km downstream of the sub-reach). Seepage meters (see Table 2), piezometers, and temperature sensors were installed at 36 points.

A spatial autocorrelation analysis shows that seepage rates are clustered with p-value 0.04 (for a z-score of 2.05) which means there is less than 5% likelihood that this clustering could be the result of random chance. The average seepage rates are 2.6 g/min at the left, 7.6 g/min at the center and 9.4 g/min at the right bank of the sub-reach. This implies that lower seepage rates are clustered on the left bank (Figure 16). The topography of right bank is steeper. It might be possible that the vertical hydraulic gradient between the river and the

unconfined aquifer is lower at the left bank in comparison to the center and the right bank, or even directed downwards.

Table 2: Statistics of seepage rates obtained from installing seepage meters at the finer scale along Sub-reach A, Wolf River

Number of Data	Minimum Rate (g/min)	Maximum Rate (g/min)	Mean Rate (g/min)	Median Rate (g/min)	Standard Deviation (g/min)	No. of losing points	No of points below 5 g/min
36	-10.5	19.4	6.0	2.9	7.6	7	20

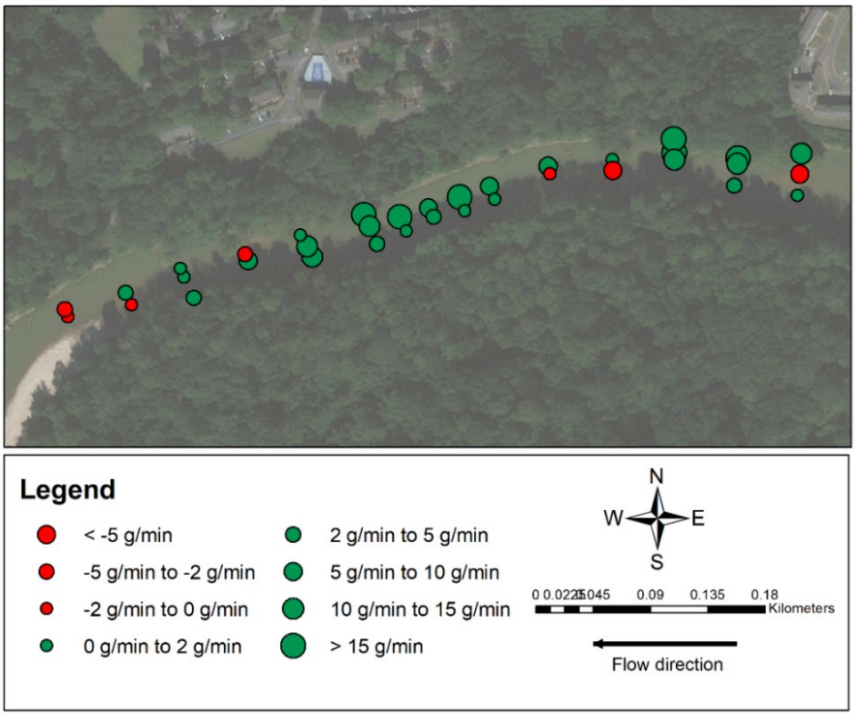

Figure 16. Spatial distribution of seepage rates obtained from installing seepage meters at the finer scale along Sub-reach A, Wolf River.

Differential stream gaging was conducted at this location on 8/10/2020, over a 930 m-long reach that incorporates the seepage grid. Performing this nearly a year later was due to a pause in research by the contracting sponsor followed by wet-weather stream conditions. The upstream discharge was 8.59 m^3/s and the downstream discharge was 8.61 m^3/s. Given the measurement uncertainty of 3% in flows, this difference is negligible; thereby, indicating no determinable gain or loss. There is a 96% overlap between the two normal distributions centered about each measured flow rate which indicates that these two discharges are not significantly different. This might be due to presence of both losing and gaining areas within

the study reach, as suggested by the seepage meter grid data, or else the reach length is too short to capture any losing/gaining signal. It might also be the case that this area is gaining less than it would from the local water table due to the influence of a local water table depression as discussed in the first phase, but data over more sub-reaches would be needed to ascertain this hypothesis.

Area Near the Closed Landfill in Shelby Farms (Sub-reach B). This location lies near the landfill in Shelby Farms Park, where previous studies have identified and examined a breach in the confining layer (Graham and Parks, 1986; Parks, 1990; Waldron et al., 2009; Schoefernacker, 2018). The water table maps for the unconfined aquifer (Narsimha, 2007; Ogletree, 2016; Schoefernacker, 2018) as well as the potentiometric map for the confined aquifer show depressions immediately north of this sub-reach. Waldron et al. (2009) conducted an S-wave reflection seismic survey in this area, verifying the presence of a breach. Bradley (1991) observed a downstream decrease in the discharge of the Wolf River in this area while conducting series of discharge measurements, but it was within instrumentation error.

The finer-scale seepage meter data were collected at this location on October 4, 2019. The mean river discharge and stage on that day were 6.57 m^3/s and 0.83 m, respectively, at the "USGS 07031650 Wolf River at Germantown, TN" gage (located 4 km upstream), while they were 8.12 m^3/s and 4.07 m, respectively, at the "USGS 07031740 Wolf River at Hollywood St at Memphis, TN" gage (locate 18.5 km downstream). The grid in this area consists of five rows to better understand the spatial variability of measurements across the transects. Seepage meters (Table 3) and piezometers were installed at 42 points.

The spatial autocorrelation analysis shows that seepage rates are randomly distributed with p-value 0.69 (for a z-score of 0.39). The average seepage rates are 13.2 g/min, 17.1 g/min, 17.7 g/min, 15.1 g/min, and 6.62 g/min from the left to the right bank of the sub-reach.

The right bank seems to be gaining less, which might be due to the presence of a depression in the unconfined water table on that side; hence, reflecting the effects of the known breach as shown in Figure 17.

Table 3: Statistics of seepage rates obtained from installing seepage meters at the finer scale along Sub-reach B, Wolf River.

Number of Data	Minimum (g/min)	Maximum (g/min)	Mean (g/min)	Median (g/min)	Standard Deviation (g/min)	No. of losing points	No of points less than 5 g/min
45	-0.8	27.6	13.7	16.1	7.6	2	9

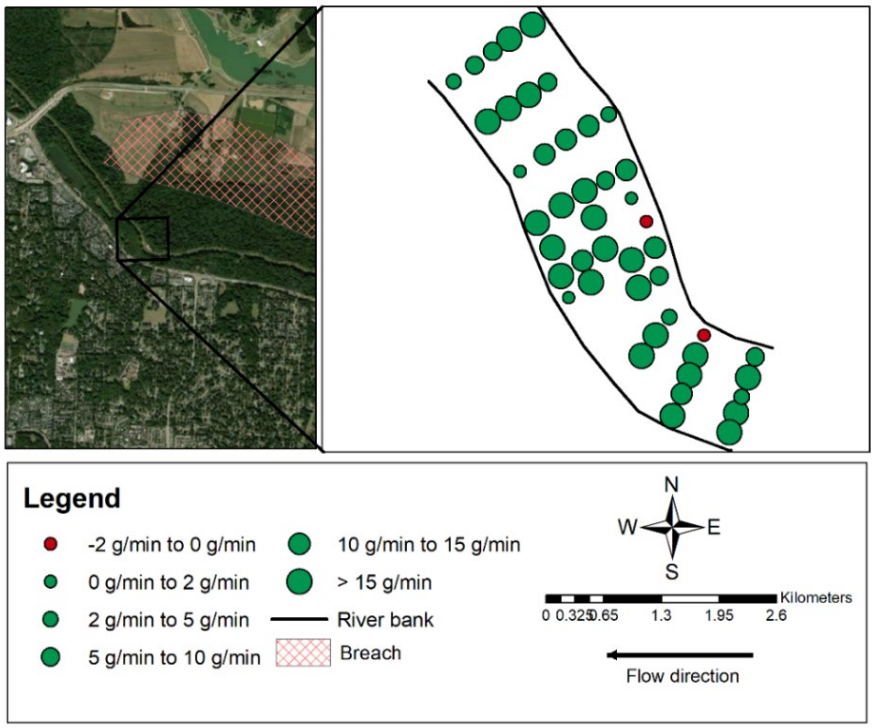

Figure 17. Spatial distribution of seepage rates obtained from installing seepage meters at the finer scale along Sub-reach B, Wolf River.

Differential stream gaging was conducted at this location on 8/11/2020, over a 970 m-long reach which includes the above seepage grid. The upstream discharge was 8.36 m^3/s and the downstream discharge was 8.55 m^3/s. The difference of 0.19 m^3/s in discharge lies within the measurement uncertainty of 3%, with a 45% overlap between the normal distributions, which suggest that the two discharges are not significantly different. Thus, it can be concluded that this reach is also neither gaining nor losing. The existing, known breach near

the right bank might influence this reach minimally, or else the reach is losing to the breach, while at the same time gaining on its left bank such that there exists no overall net gain.

Area near Lansdowne Park at Germantown (Sub-reach C). Seepage meter data were collected on September 27, 2019. The mean river discharge and stage on that day were 7.41 m^3/s and 0.86 m, respectively, at the "USGS 07031650 Wolf River at Germantown, TN" gage (3.8 km downstream). This area is an outcrop zone (recharge zone) for the Memphis aquifer according to Larsen (personal comm.) and Parks (1990), and thus conditions should be losing. Seepage meters (Table 4), piezometers, and temperature sensors were installed at 42 points.

Table 4: Statistics of seepage rates obtained from installing seepage meters at the finer scale along sub-reach C, Wolf River.

Number of Data	Minimum (g/min)	Maximum (g/min)	Mean (g/min)	Median (g/min)	Standard Deviation (g/min)	No. of losing points	No of points less than 5 g/min
42	-17.6	22.0	9.7	11.7	10.5	6	12

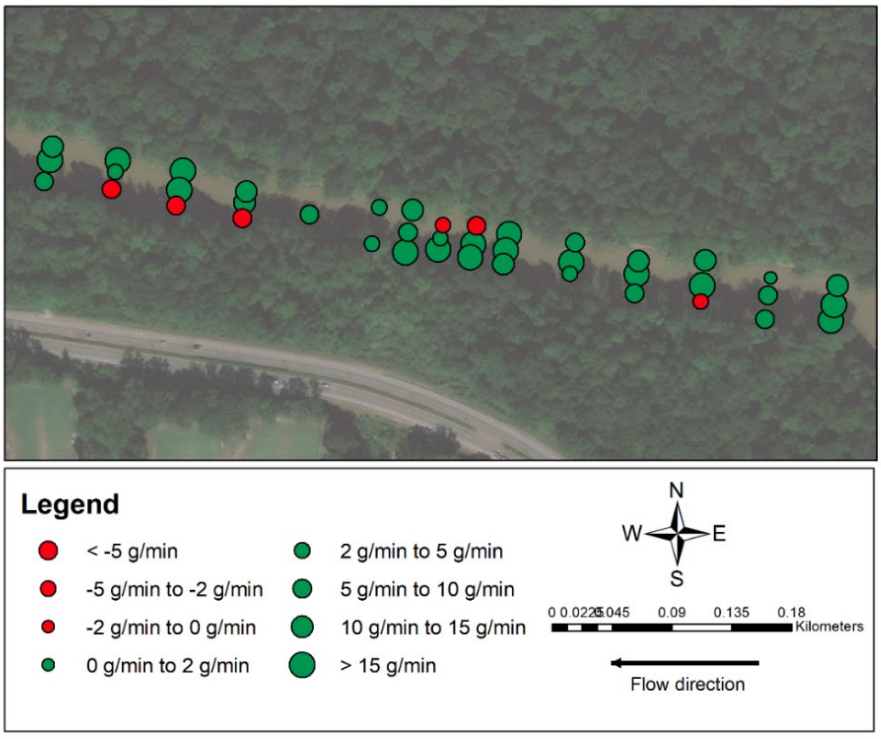

Figure 18. Spatial distribution of seepage rates obtained from installing seepage meters at the finer scale along Sub-reach C, Wolf River.

The spatial autocorrelation analysis shows that seepage rates are randomly distributed with p-value 0.35 (for a z-score of -0.92). The average seepage rate is 5.0 g/min at the left, 14.9 g/min on center, and 9.0 g/min on the right bank of the sub-reach (Figure 18).

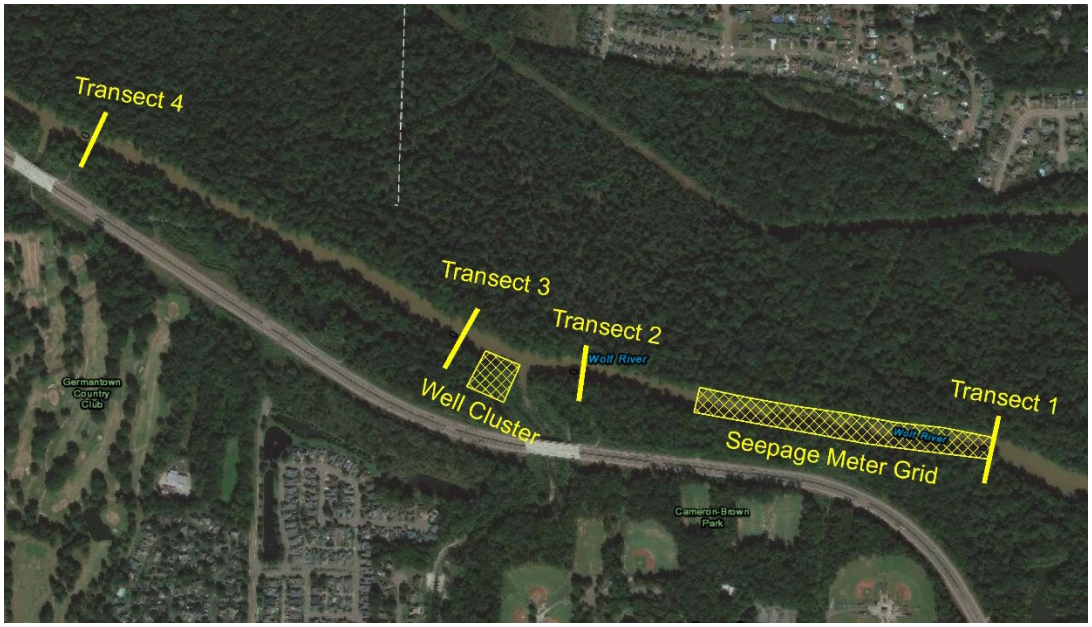

Figure 19. Location of well cluster, seepage meter grid, and stream gaging transects along the reach near Lansdowne Park in Germantown (Sub-reach C).

Differential stream gaging was conducted at this location on 8/6/2020, in a reach of length 820 m between Transects 1 and 2 in Figure 19. The upstream discharge was 9.74 m^3/s and the downstream discharge was 9.31 m^3/s. Even though the difference of 0.43 m^3/s lies within the measurement uncertainty of 3%, these two discharges are significantly different with only a 14% overlap in area between the two normal distributions. Another differential stream gaging was also conducted on 8/5/2020, over a reach of length 890 m, located immediately below, between Transects 3 and 4 in Figure 19. The upstream discharge was 9.94 m^3/s and the downstream discharge was 9.85 m^3/s. With 75% overlapping area, these two discharges are not significantly different.

The discharges observed at these four transects were compared with that recorded at the gage 'USGS 07031650 Wolf River at Germantown, TN' which lies about 3.8 kilometers downstream from Transect 1 (Table 5). Analysis of 52 USGS stream gage records conducted

over the last 15 years at the USGS gaging station during low flow conditions ($Q < 14$ m^3/s) shows that the discharge estimated from the rating curve tends to slightly overestimate the true discharge. All four measurements in the vicinity of this gage show discharges that are quite larger than those reported at the gage (3.8 to 7.8 % larger), even though the surface water tributaries between the transects and the gage were all dry during the measurement windows. These observations suggest that the Wolf River is most likely losing water between Lansdowne Park and the USGS gaging station. Comparing with our First Phase analyses, this portion of the river also displays lower seepage rates, corresponding to a cold spot area (Figure 13).

Table 5: Discharge obtained from precision stream gaging using Ott current meters, and discharge recorded simultaneously at 'USGS 07031650 Wolf River at Germantown, TN'.

Date		Gaged (m^3/s)	USGS (m^3/s)	Relative difference (%)
08.06.2020	Transect 1:	9.74	8.98	7.8
	Transect 2:	9.31	8.97	3.6
08.05.2020	Transect 3:	9.94	9.44	5.1
	Transect 4:	9.85	9.43	4.3

Discussion. A high spatial variation in vertical exchange fluxes is observed at the finer spatial measurement scale (Figures 16, 17, and 18). Gaining and losing water conditions are found simultaneously at each sub-reach. Again, this large spatial variability might be due to heterogeneity in hydraulic conductivity or vertical hydraulic gradient, local hyporheic exchange (that usually occurs in upper layers of unconsolidated streambeds), and the fact that the seepage measurements are at a very small spatial scale. Still, the seepage rate measurements at the finer scale do show a smaller dispersion as compared to those over the full reach, which suggests that there is some spatial structure at the sub-reach scale. The data collected with seepage meters do not give us enough confidence to state that any sub-reach is predominantly losing.

Seepage rates at Sub-reach A show strong patterns on the left bank, whereas in sub-reaches B and C the seepage rates are randomly distributed. Murdoch and Kelly (2003) installed seepage meters in a sandy channel streambed and found that seepage fluxes were highest at the center of the stream, decreasing towards the banks. A similar pattern was observed in most of the cases, with seepage rates that are relatively lower near the banks than at the center of the stream.

The differential stream gaging data only show small differences between the upstream and downstream cross-sections, in most of the cases. This might be due to simultaneous gain of water from one bank and loss to the other bank where there exists a breach, or else the reach lengths are too short to capture any losing/gaining signal. Due to the fact that the Wolf River in Shelby County area is a gaining system overall, it is also possible that there are indeed breaches near the sub-reaches A and B, that cause those locations to be gaining less water, as compared to fully gaining areas. Demonstrating this would require applying the differential stream gaging technique over the whole 49-km reach, though. Doing so using current meters is not pragmatic though, as it takes a full day to complete a single cross-section. It is recommended to gage with an Acoustic Doppler current profiler (ADCP) for future research, using multiple passes at each transect. Even though it is less accurate that a current meter, for a single measurement, an ADCP can minimize the total time needed to complete this effort, while performing multiple passes helps increase accuracy.

Comparison with Other Techniques

Mini Piezometers. At Sub-reach A, mini-piezometer readings were used to compute two vertical hydraulic gradients (VHGs) at each location, between the streambed, and 30 cm and 80 cm depths below it. There was no correlation between two VHG ($r = -0.015$). This might be because the impact of local hyporheic flow is higher near the surface or is just due to errors and inconsistencies in measurement. The correlation between these two VHGs (at 30

cm and 80 cm depths) and seepage rates are 0.20 and 0.053, respectively. The VHG was computed between the streambed and a depth of 100 cm in Sub-reaches B and C, and correlation with the seepage rate was 0.27 and 0.22, respectively. These results imply that there is no correlation between seepage meter and mini-piezometer measurements.

Temperature Sensors. In Sub-reach A, temperatures were recorded at depths of 30 cm and 80 cm below the streambed (Figure 20), using iButtons, at the same locations where seepage meters were also installed. There was no correlation between the seepage rates and the instantaneous temperatures or the temperature difference between the two depths. There is a convincing correlation between the temperature recorded at the two depths, with a Pearson correlation coefficient (r) value of 0.83. In most of the cases, the temperature at a depth of 30 cm is higher than that at 80 cm, which is expected during summertime. Still, because we do not know a priori how temperature would behave at 30 cm and 80 cm depths under clear gaining and losing conditions, we were not able to discriminate with these temperature data. Moreover, the observed differences in temperature are less than 1° C, which lies within the measurement accuracy of the iButtons that were used (± 1° C).

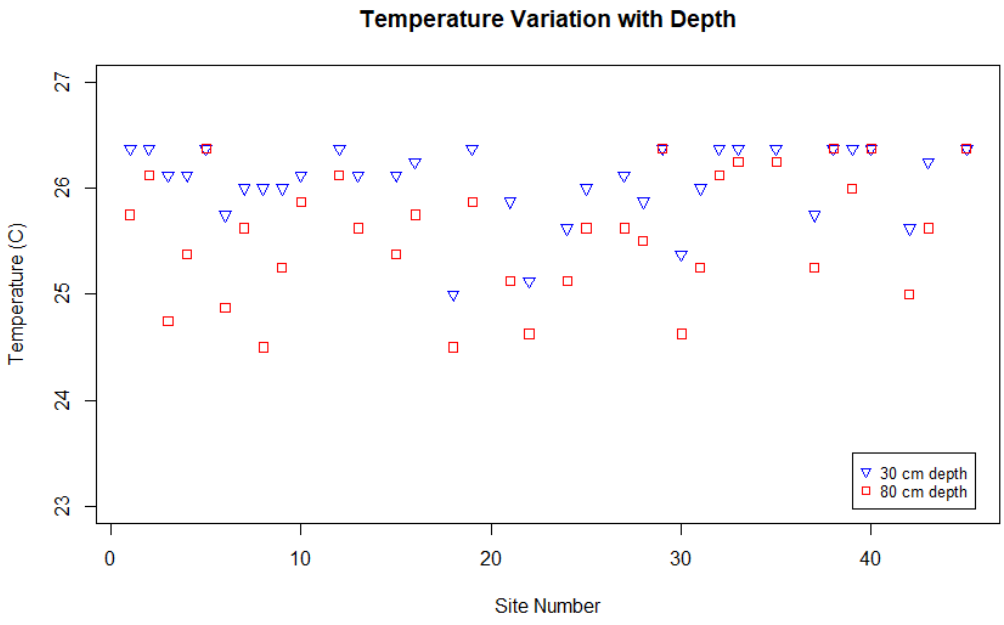

Figure 20. Temperatures measurements at two different depths in Sub-reach A, Wolf River

In Sub-reach C, temperatures were recorded at depths of 20 cm, 60 cm, 100 cm below the streambed, as well as in the mid-section of the water column, during daytime (between 8 a.m. and 3 p.m.). The surface water temperatures measured during the morning are lower than those during midday and the afternoon, as is implicit in Figure 21 (we started measuring temperature at Site 1 in the morning, and finished at Site 45 in the afternoon). Nonetheless, the patterns in temperature at depths of 20, 60 and 100 cm remain similar throughout the day. This means that the increase in surface water temperature is not affecting the temperature at any depth, indicating gaining conditions. When comparing surface water temperature with temperature at 100 cm depth, the difference is less than 1° C for the first ~10 sites, sampled in the morning, but then increases to an average of about 2° C, at locations where measurements were conducted later.

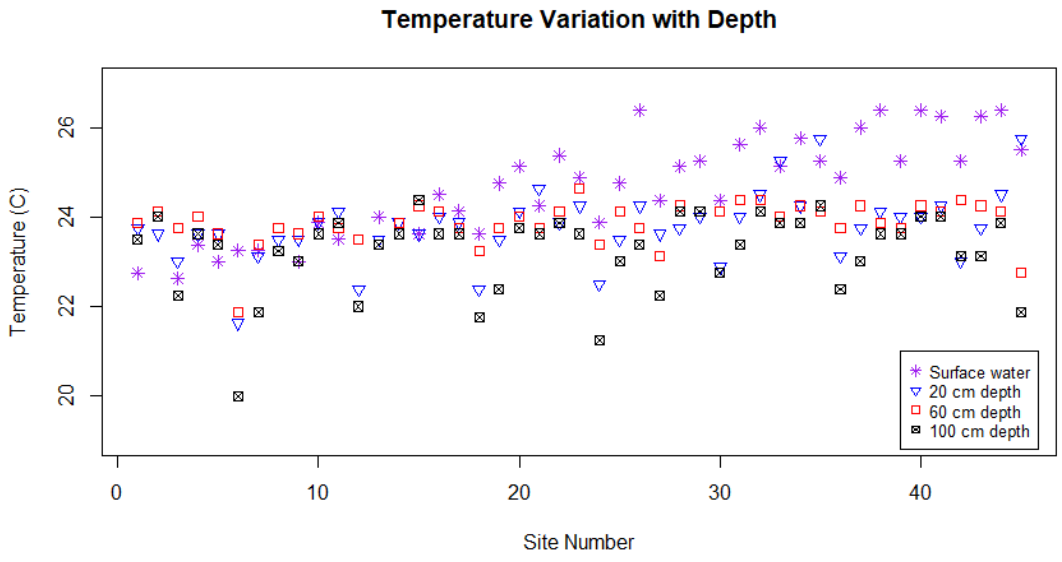

Figure 21. Temperature profile obtained by installing temperature sensors at three different depths below the streambed and in the surface water column in Sub-reach C, Wolf River

In both sub-reaches, the temperature recorded at the shallow depth is almost always higher than the deeper temperature, which would be expected under gaining conditions

during summertime. Like seepage rates, temperature is a small-scale, near-surface measurement, which can be unduly influenced by other small-scale factors.

Potential Errors/Issues with the Methodology

Seepage Meters. Seepage meters can measure the seepage rate well in static water. In the case of flowing conditions though, especially in rivers with moving sandy bottoms, there are a lot of variables that can affect the observed seepage rate. Most potential errors were minimized during design of the seepage meter, such as: using a shelter bucket with hole, selecting a barb bell valve, minimizing connections, constrictions, and bends to lessen friction losses, etc. Some other issues such as scouring around the seepage bucket (a few inches from the top), influence of human movement around the measurement area, etc. were observed or suspected during data collection. The seepage meters were deployed at 523 data points (including first and second phases) and for about 40% of the measurements, the bags gained more than 1000 g of water. Flow into the bag decreases sharply when it is nearly full (Murdoch and Kelly, 2003). Therefore, there is a possibility that total possible flux was underestimated in some of the cases. The impacts of these possible/suspected errors and biases are unknown and difficult to quantify.

Temperature Sensors. The iButtons used to measure temperature in this study have an accuracy of ±1° C. The measured temperature differences were low (Figure 20 and 21), and some of them could be due to measurement accuracy of the iButtons. Due to hyporheic mixing of surface water and groundwater in unconsolidated sediments like those composing the Wolf River riverbed, temperatures at shallow depths are influenced by surface temperature. Also, the fact that surface water can enter the streambed earlier during hyporheic exchange might also affect the temperature profile, due to the expected diel changes in surface water temperature. The temperatures recorded in this study were basically

instantaneous; continuous measurements of temperature (over at least 24 hours) would be required to distinguish losing/gaining conditions, due to above mentioned issues.

Mini Piezometers. Even though mini-piezometers are the most direct method to physically measure the direction of vertical exchange flux, they could introduce rather large errors due to inconsistencies in tape reading, effects of water velocity, etc. Placing a hollow bucket around the pipe when measuring the surface water head outside the piezometer and using steel tape with chalk did help in minimizing some of the possible errors. But still, there were difficulties and inconsistencies with the tape readings. As head differences were very low at most locations (only a few millimeters at most), it is clear from the above issues that the data obtained with mini-piezometers are not good enough to draw conclusions regarding vertical water flux.

Third Phase: Monitoring River Stage and Groundwater Levels

The stilling well in the river, and two groundwater monitoring wells – one screened into the unconfined aquifer, the other in the confined aquifer - were installed in an area near Lansdowne Park in Germantown (Figure 19). The borehole log shows a 55 ft (17 m) thick clay layer (UCCU) at this location starting at a depth of 50 ft (15 m). At least at this specific point, this evidence disagrees with the notion that this river segment lies in an outcrop zone, as suggested by Parks (1990) and Larsen (personal comm.). However, this does not discard the potential existence of a breach or an outcrop zone somewhere nearby, due to the high spatial heterogenity in clay thickness as evident, for example, in the area near the Closed Landfill in Shelby Farms (Parks and Mirecki, 1994; Gentry et al., 2006). The well data for this research were collected between May and August 2020 and are shown in Figure 22.

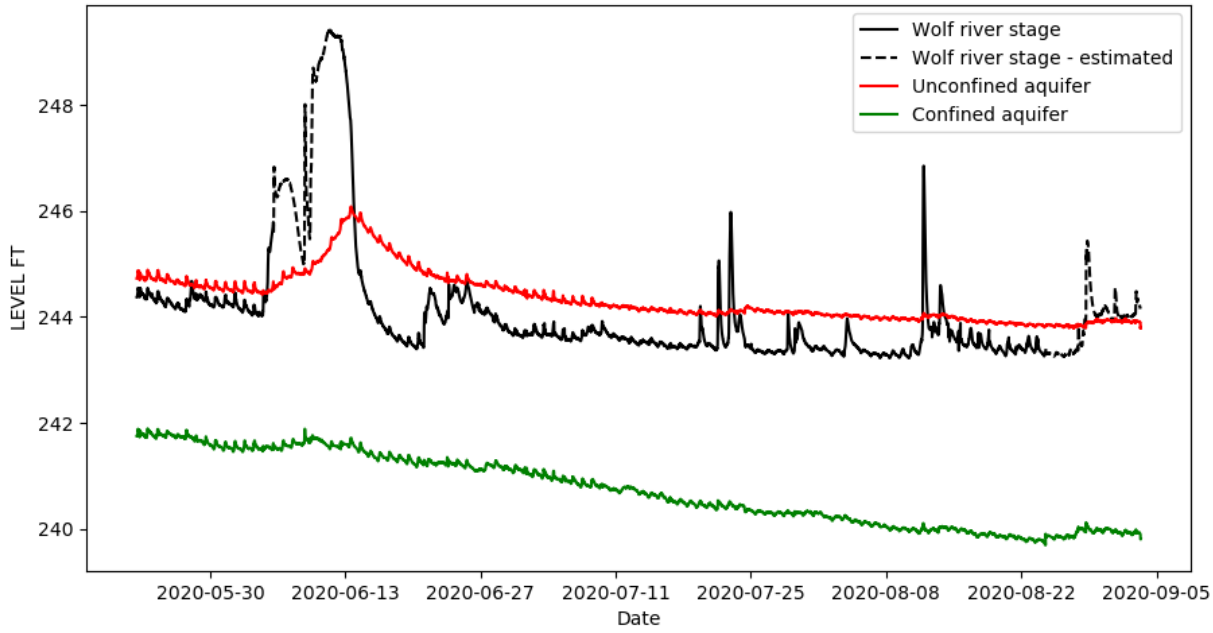

Figure 22. Comparison of time series for the Wolf River stage, the elevation of the water table in the unconfined aquifer, and the potentiometric surface of the confined aquifer, from wells located near Lansdowne Park in Germantown. Note: water levels are measured in feet.

A small-scale fluctuation at the diel time scale can be observed in all of the water levels (Figure 22). We hypothesized that this is due to the process of barometric compensation that is applied to obtain the water levels inside the wells. This is performed by subtracting atmospheric pressure, as recorded by a pressure sensor (Solinst Barologger) located outside the well, from the total pressure logged by the transducers inside the wells. As the wells have an airtight lid which does not allow the inside pressure to equilibrate quickly, it will be slightly different and fluctuate less than atmospheric pressure. To validate this point, barometric compensation was conducted using atmospheric pressure as recorded both inside and outside a well (Figure 23). The resulting water levels are slightly different (up to 0.2 ft, or 6 cm). Therefore, the small fluctuations seen in Figure 22 are indeed an artifact of the barometric compensation process. For future studies, it would be better to record air pressure inside the wells with Barologgers, if the well is airtight, along with total pressure with a transducer, to compute water levels more accurately, or use a vented transducer.

The water levels obtained with a Barologger inside the well still display small diel fluctuations (dark curve in Figure 22), though with smaller undulations than the ones in Figure 22. These might be due to some unknown error in barometric compensation, or might be actual water level fluctuations, e.g., due to evapotranspiration. These cycles need more detailed investigation for further analysis.

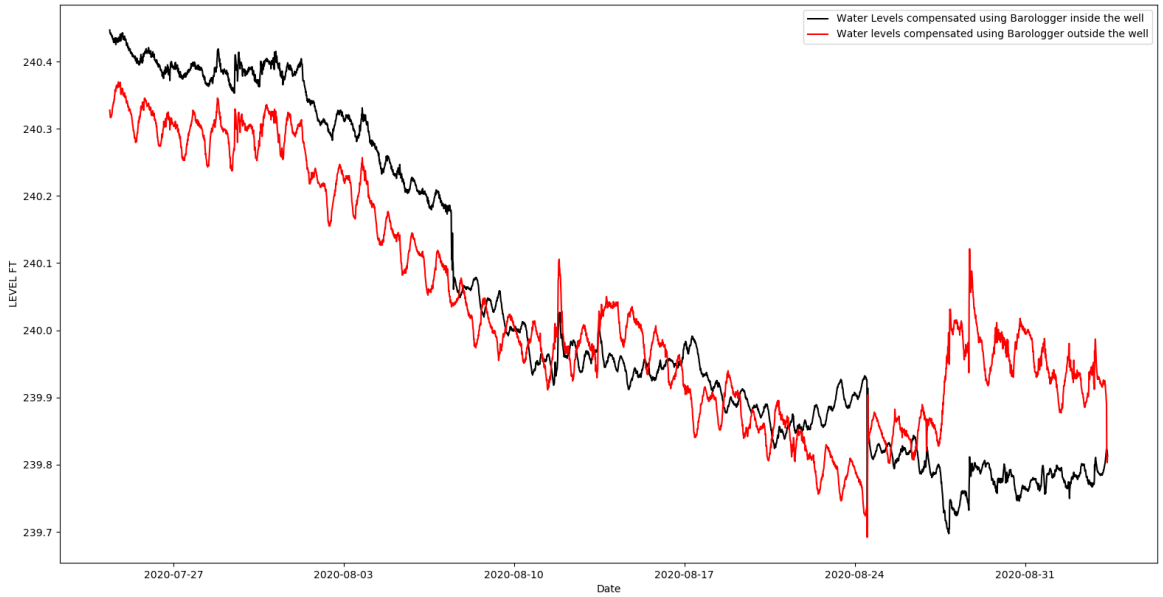

Figure 23. Comparison of water levels obtained from barometric compensation using the Barologger inside the well versus outside the well. Note: water levels are measured in feet.

Along the reach near Lansdowne Park, the river should be gaining from the unconfined aquifer during base flow conditions, as seen in Figure 22. During the larger flood events captured in our data, the river stage increases abruptly, an effect that can be also noticed in the unconfined aquifer water level, but with a delayed and smoothed response. The confined aquifer did not show any significant response to such larger events, during which the river temporarily converts into a losing system. There is no response in any of the aquifers to the smaller, shorter flood events. There might be a case that the unconfined aquifer is only influenced from such larger flooding events which can temporarily convert the river into a losing system. Therefore, it is recommended that the connection between the aquifers and the river be investigated over a longer period, including the high flow period

(during winter) when the river should be mostly losing. There is also a possibility that the river could be gaining from one bank while simultaneously losing on the other bank. It is clear that well data for a single point, on only one side of the river are not sufficient; consequently, further investigation is required at more cross-sections, with more observation wells along both banks of the river. It would be better to install multiple wells in a transect covering both banks; however, this is not pragmatic due to expensive nature of well drilling.

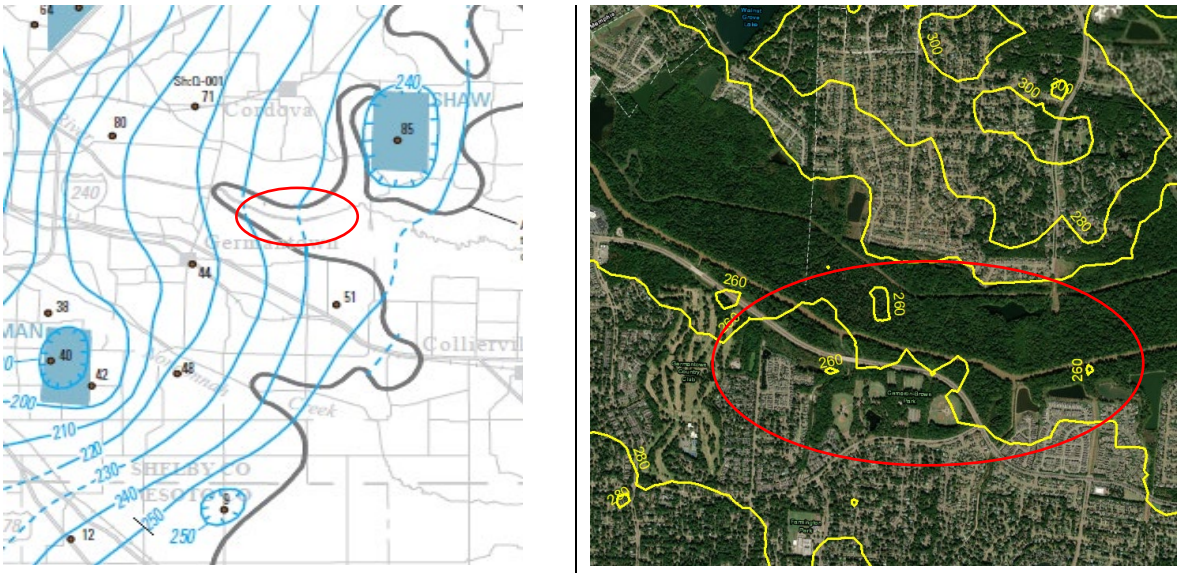

A

Clipped from Kingsbury (2018)

B

Created using Ogletree (2016) data

Figure 24. Comparison of potentiometric surface map and water table map for the confined aquifer (A) and the unconfined aquifer (B), showing the area of interest. Note: contours are measured in feet.

Kingsbury (2018) and Ogletree (2016) created maps of the potentiometric surface of the confined aquifer and water levels of the unconfined aquifer, respectively, using water levels collected between September and November 2015 (Figure 24). They found potentiometric water level elevations of 240 ft (approx., or 73 m) and unconfined aquifer water elevations of 260 ft (approx., or 79 m) in the area near Lansdowne Park in Germantown. The water table map created by Narsimha (2007) also gives elevation similar to those of Ogletree (2016). Comparing these levels, it could be concluded that there is a

vertical downward gradient between the two aquifers with a head difference of about 6 m (20 ft) in this vicinity. It should be noted though that both Kingsbury (2018) and Ogletree (2016) created these water level contour maps with limited data, using interpolation methods. However, the observed water levels at Lansdowne Park indicate a head difference of about 0.9 m (3 ft). The unconfined water levels are about 15 ft below the interpolated data obtained from the Ogletree (2016) water level map, which is a significant difference. Ogletree (2016) compared his water table map to previous historical maps, concluding that they are similar except in those areas where well control changed. The observed differences between present water levels, as observed in this study, and those from historical map is possibly due to the addition of new data points as discussed by Ogletree (2016). However, it should be noted that this is a comparison of data measured locally, with historical regional contours at a broader scale.

CONCLUSIONS

The Memphis aquifer is a major source of water in Shelby County, which needs to be protected from contamination due to inter-aquifer water exchange through naturally occurring breaches in the intervening aquitard. The number, size, and locations of these breaches is not well known, and a better description would help protect the Memphis aquifer. This research was carried out along one of the rivers in Shelby County, the Wolf River, in an attempt to locate unknown breaches in located near the river by investigating GW-SW interactions under the assumption that the presence of a nearby breach should affect the vertical exchange flux in the streambed.

First, seepage meters were used to measure vertical flux every 100 m along the 49 km-long lower reach of the Wolf River. Initial results show a few losing points separated by gaining points, but did not depict obvious losing patterns. Spatial analyses of the data indicated spatial patterns in the data. Based on the results three sub-reaches were chosen for

in-depth study at a finer spatial scale using a suite of methods: comparing seepage meters, differential stream gaging, piezometers, and temperature sensors. The finer scale observation of seepage rates shows that gaining and losing points occurs simultaneously within a sub-reach, which makes it difficult to confirm losing conditions.

The seepage meter data display a high spatial variation of vertical exchange flow at both studied spatial scales (full reach and sub-reaches). Comparing seepage rates with piezometer and temperature profile data yields low correlation values, which could be due to the issues associated with each individual method and its application. The temperature at shallow depths was almost always higher than the deep temperature, which is expected in summertime; however, the range of variation of the expected temperature profile in gaining and losing conditions is unknown, as compared to the accuracy of the temperature sensors used (iButtons) such that it is difficult to draw firm conclusions.

Approaching problem at the reach scale, the data from differential stream gaging at different locations provide better understanding of net, integrated loss or gain. The differences in discharge for the sub-reaches downstream of Austin Peay Highway and near the Closed Landfill in Shelby Farms were small against the uncertainty in discharge measurement, while we measured a statistically significant difference in the reach near the Lansdowne Park. There might be several reasons that explain why for these reaches the difference of discharge is small such as, decreased influence of the unconfined aquifer, losing from one bank while gaining from other, short reach length to capture losing/gaining signal, etc. When comparing the discharge near Lansdowne Park to the continuous measurement at the USGS gage (1.7 km to 3.8 km downstream), it was observed that the gaged discharges were significantly higher (3.6 to 7.8 % higher) than the discharge recorded by USGS gage, which suggests that the Wolf River is mostly losing along these reaches.

Data collected from monitoring wells along the reach near Lansdowne Park in Germantown (over a limited timeframe, though) show a different picture: that the river gains during base flow condition and temporarily converts into a losing system during large flooding events. The confined aquifer did not show any significant response to the flooding events during the study period. The response of the confined aquifer needs further investigation using data over a longer duration. When comparing the water levels observed in the well cluster with the water table maps in the literature, significant differences in the unconfined aquifer water levels were found. Other sub-reaches need to be further investigated using additional and improved methodologies to confirm losing conditions, before drilling observation wells. Given that different lines of evidence suggest the possibility of gain in one bank, but loss in the other, it would be better to have well transects covering both banks of the river.

The main objective of this research was to locate losing areas along an extensive reach of the Wolf River so that these can be further investigated to confirm or discard the presence of any nearby breach. Even though installing seepage meters, a point-scale measurement, every 100 m over such a long reach undoubtedly raises issues related to the observation scale, indirect spatial patterns were observed that helped us select areas to focus the study. The simultaneous application of multiple methods at the sub-reach scale did not reach conclusions; however, it provides a basis for future application of these methods in unconsolidated sediment streambeds, such as the Wolf River.

In the end, the idea of identifying potential aquitard breach locations near the river through investigation of GW-SW interactions remains promising, but there is a clear need for finding new techniques or refining the ones used in this study in order to better predict GW-SW exchange at varying scales while accounting for other factors that can impact the results. Some of the methods with a larger resolution that can be used for future research are thermal

profiling, aerial infrared photography, and differential discharge runs using ADCP with multiple passes.

RECOMMENDATIONS FOR FUTURE WORK

Seepage meters

The seepage meter can still be a good option for quantifying GW-SW interactions at the point scale, notwithstanding the issues related to its installation and data measurement technique. According to the issues identified during fieldwork, the following recommendations can be drawn for future application of seepage meters in conditions such as those found in the Wolf River:

1. In unconsolidated sediments, it is difficult to get a complete seal of the seepage bucket due to scouring around the container. Fellows & Brezonik (1980) suggested using taller seepage meters to reduce this error. In our research, 30 cm tall buckets were used, but we observed slight scouring at the top of the bucket in some cases. Thus, it is recommended to use larger buckets in future studies, realizing that it might be challenging to drive them into the riverbed.
2. Seepage bags were installed and allowed to sample for one hour, over which many of them ended up filling, so that total possible flow was not obtained in some cases. Flow into the bag decreases sharply when it is nearly full (Murdoch and Kelly, 2003). Thus, using shorter installation times (e.g., only 30 minutes) can minimize this issue in future work.
3. If the purpose of the study is to quantify actual seepage rates precisely, then it is recommended to obtain the calibration coefficient for the catheter bags (Rosenberry and LaBaugh, 2008), as they have a fairly thick wall, that could restrict the flow, leading to underestimation of the seepage rate.

4. Using a larger diameter pipe to connect the seepage bag to the bucket, and use of the seepage bag with walls as thin as possible can minimize resistance due to friction and wall effects, respectively (Rosenberry and LaBaugh, 2008).

Temperature Sensors

The instantaneous temperature data collected in this study were not conclusive. As it is not pragmatic to continuously measure temperature at a large number of sampling points, its behavior should be first studied in detail at a few gaining and losing locations, so that instantaneous temperature data can then be related to the direction of vertical flow. Hence, for future work it is recommended to measure the vertical temperature profile over a longer duration (at least 24 hours), to understand the patterns of the temperature profile for different scenarios, which could then be correlated with instantaneous temperature profiles to obtain the direction of vertical exchange flux. It is also recommended to measure the temperature profile to deeper depths to observe clear differences to help in minimizing effects of hyporheic exchange flow, which is stronger at the near surface.

Mini Piezometers

A reliable technique is needed to minimize the errors generated due to inconsistencies in tape readings. Use of an oil water manometer (Kennedy et al., 2007) with mini piezometers can resolve this issue, even though this device is a much more expensive to set-up.

LITERATURE CITED

Anderson, M.P., 2005. Heat as a Ground Water Tracer. Groundwater 43:951–968.

Baxter, C., F. Hauer, and W. Woessner, 2003. Measuring Groundwater–Stream Water Exchange: New Techniques for Installing Minipiezometers and Estimating Hydraulic Conductivity. Transactions of The American Fisheries Society - TRANS AMER FISH SOC 132:493–502.

Becker, M.W., T. Georgian, H. Ambrose, J. Siniscalchi, and K. Fredrick, 2004. Estimating Flow and Flux of Ground Water Discharge Using Water Temperature and Velocity. Journal of Hydrology 296:221–233.

Blanchfield, P.J. and M.S. Ridgway, 1996. Use of Seepage Meters to Measure Groundwater Flow at Brook Trout Redds. Transactions of the American Fisheries Society 125:813–818.

Boano, F., J.W. Harvey, A. Marion, A.I. Packman, R. Revelli, L. Ridolfi, and A. Wörman, 2014. Hyporheic Flow and Transport Processes: Mechanisms, Models, and Biogeochemical Implications. Reviews of Geophysics 52:603–679.

Boiten, W. and I.H.E. Hydrometry, 2000. Delft Lecture Note Series. AA Balkema, Rotterdam.

Bouyoucos, G.J., 1915. Effect of Temperature on Movement of Water. Journal of Agricultural Research 5:141.

Bradley, M.W., 1991. Ground-Water Hydrology and the Effects of Vertical Leakage and Leachate Migration on Ground-Water Quality near the Shelby County Landfill, Memphis, Tennessee.

Bradshaw, E.A., 2011. Assessment of Ground-Water Leakage through the Upper Claiborne Confining Unit to the Memphis Aquifer in the Allen Well Field, Memphis, Tennessee. University of Memphis, Memphis, TN.

Brahana, J. and R. Broshears, 2001. Hydrogeology and Ground-Water Flow in the Memphis and Fort Pillow Aquifers in the Memphis Area, Tennessee. Water-Resources Investigations Report 89:4131.

Broughton, A.T., R.B. Van Arsdale, and J.H. Broughton, 2001. Liquefaction Susceptibility Mapping in the City of Memphis and Shelby County, Tennessee. Engineering Geology 62:207–222.

Brunke, M. and T. Gonser, 1997. The Ecological Significance of Exchange Processes Between Rivers and Groundwater. doi:10.1046/j.1365-2427.1997.00143.x.

Calver, A., 2001. Riverbed Permeabilities: Information from Pooled Data. Groundwater 39:546–553.

Carmichael, J.K., J.A. Kingsbury, D. Larsen, and S. Schoefernacker, 2018. Preliminary Evaluation of the Hydrogeology and Groundwater Quality of the Mississippi River Valley Alluvial Aquifer and Memphis Aquifer at the Tennessee Valley Authority Allen Power Plants, Memphis, Shelby County, Tennessee. Reston, VA. doi:10.3133/ofr20181097.

Carter, R. W., & A.I.E., 1963. Accuracy of Current Meter Measurements N. J. Hydraulics

Division, Proc. ASCE 4, no. 1 (1963), pp. 105–115.

Cey, E.E., D.L. Rudolph, G.W. Parkin, and R. Aravena, 1998. Quantifying Groundwater Discharge to a Small Perennial Stream in Southern Ontario, Canada. Journal of Hydrology 210:21–37.

Constantz, J. and D.A. Stonestrom, 2003. Heat as a Tracer of Water Movement near Streams. US Geological Survey Circular:1–96.

Le Coz, J., P.. Bechon, B. Camenen, and G. Dramais, 2014. Quantification of the Uncertainties Related to Velocity-Area Streamgauging Data. La Houille Blanche - Revue Internationale de l'eau:31–39.

Le Coz, J., B. Camenen, X. Peyrard, and G. Dramais, 2012. Uncertainty in Open-Channel Discharges Measured with the Velocity–Area Method. Flow Measurement and Instrumentation 26:18–29.

Criner, J.H., P.-C.P. Sun, and D.J. Nyman, 1964. Hydrology of Aquifer Systems in the Memphis Area, Tennessee. U.S. Gov't. Printing Office. doi:10.3133/wsp1779O.

Dieter, C.A., M.A. Maupin, R.R. Caldwell, M.A. Harris, T.I. Ivahnenko, J.K. Lovelace, N.L. Barber, and K.S. Linsey, 2018. Estimated Use of Water in the United States in 2015. Reston, VA. doi:10.3133/cir1441.

EN ISO 748, 2007. ISO 748:2007 Hydrometry: Measurement of Liquid Flow in Open Channels Using Current-Meters Or Floats. International Organization for Standardization. https://books.google.com/books?id=GtUecgAACAAJ.

Essaid, H.I., C.M. Zamora, K.A. McCarthy, J.R. Vogel, and J.T. Wilson, 2008. Using Heat to Characterize Streambed Water Flux Variability in Four Stream Reaches. Journal of Environmental Quality 37:1010–1023.

Fellows, C.R. and P.L. Brezonik, 1980. SEEPAGE FLOW INTO FLORIDA LAKES1. JAWRA Journal of the American Water Resources Association 16:635–641.

Fulford, J., Sauer, V., 1986. Comparison of Velocity Interpolation Methods for Computing Open-Channel Discharge. U.S. Geological Survey Water-Supply Paper 2290,:139–144.

Gallo, H.G., 2015. Hydrologic and Geochemical Investigation of Modern Leakage beneath the McCord Well Field, Memphis, Tennessee. University of Memphis, Memphis, TN.

Gentry, R., L. McKay, N. Thonnard, D. Larsen, and J. Anderson, 2006. Novel Techniques for Investigating Recharge to the Memphis Aquifer. American Water Works Association.

Graham, D.D. and W.S. Parks, 1986. Potential for Leakage among Principal Aquifers in the Memphis Area, Tennessee. doi:10.3133/wri854295.

Israelsen, O.W. and R.C. Reeve, 1944. Bulletin No. 313 - Canal Lining Experiments in the Delta Area, Utah. UAES Bulletins. Paper 348.

Kalbus, E., F. Reinstorf, and M. Schirmer, 2006. Measuring Methods for Groundwater – Surface Water Interactions: A Review. Hydrol. Earth Syst. Sci. 10:873–887.

Kennedy, C.D., D.P. Genereux, D.R. Corbett, and H. Mitasova, 2007. Design of a Light-Oil Piezomanometer for Measurement of Hydraulic Head Differences and Collection of Groundwater Samples. Water Resources Research 43. doi:10.1029/2007WR005904.

Kennedy, C.D., L.C. Murdoch, D.P. Genereux, D.R. Corbett, K. Stone, P. Pham, and H. Mitasova, 2010. Comparison of Darcian Flux Calculations and Seepage Meter Measurements in a Sandy Streambed in North Carolina, United States. Water Resources Research 46. doi:10.1029/2009WR008342.

Kingsbury, J.A., 2018. Altitude of the Potentiometric Surface, 2000–15, and Historical Water-Level Changes in the Memphis Aquifer in the Memphis Area, Tennessee. Reston, VA. doi:10.3133/sim3415.

Krause, S. and A. Bronstert, 2007. The Impact of Groundwater–Surface Water Interactions on the Water Balance of a Mesoscale Lowland River Catchment in Northeastern Germany. Hydrological Processes 21:169–184.

Landon, M., D. Rus, and F. Harvey, 2001. Comparison of Instream Methods for Measuring Hydrolic Conductivity in Sandy Streambeds. Ground Water 39:870–885.

Larsen, D., R.W. Gentry, and D.K. Solomon, 2003. The Geochemistry and Mixing of Leakage in a Semi-Confined Aquifer at a Municipal Well Field, Memphis, Tennessee, USA. Applied Geochemistry 18:1043–1063.

Larsen, D., J. Morat, B. Waldron, S. Ivey, and J. Anderson, 2013. Stream Loss Contributions to a Municipal Water Supply Aquifer in Memphis, Tennessee. doi:10.2113/gseegeosci.19.3.265.

Larsen, D., S. Schoefernacker, and B. Waldron, 2017. A Report on the Results of a Groundwater Vulnerability Study in Shelby County, Tennessee. Memphis, TN. Unpublished. Personal Communication.

Larsen, D., B. Waldron, S. Schoefernacker, H. Gallo, J. Koban, and E. Bradshaw, 2016. Application of Environmental Tracers in the Memphis Aquifer and Implication for Sustainability of Groundwater Resources in the Memphis Metropolitan Area, Tennessee. Journal of Contemporary Water Research & Education 159:78–104.

Lee, D.R., 1977. A Device for Measuring Seepage Flux in Lakes and Estuaries1. Limnology and Oceanography 22:140–147.

Lee, D.R. and J.A. Cherry, 1979. A Field Exercise on Groundwater Flow Using Seepage Meters and Mini-Piezometers. Journal of Geological Education 27:6–10.

Lee, D.R. and H.B.N. Hynes, 1978. Identification of Groundwater Discharge Zones in a Reach of Hillman Creek in Southern Ontario. Water Quality Research Journal 13:121–134.

Lewis, J.B., 1987. Measurements of Groundwater Seepage Flux onto a Coral Reef: Spatial and Temporal Variations. Limnology and Oceanography 32:1165–1169.

Libelo, E.L. and W.G. MacIntyre, 1994. Effects Of Surface-Water Movement On Seepage-Meter Measurements Of Flow Through The Sediment-Water Interface. Applied Hydrogeology 2:49–54.

McCallum, J.L., P.G. Cook, D. Berhane, C. Rumpf, and G.A. McMahon, 2012. Quantifying Groundwater Flows to Streams Using Differential Flow Gaugings and Water Chemistry. Journal of Hydrology 416–417:118–132.

Murdoch, L.C. and S.E. Kelly, 2003. Factors Affecting the Performance of Conventional Seepage Meters. Water Resources Research 39. doi:10.1029/2002WR001347.

Narsimha, V.K.K., 2007. Altitudes of Ground Water Levels for 2005 and Historic Water Level Change in Surficial and Memphis Aquifers, Shelby County, Tennessee. University of Memphis.

Nyman, D.J., 1965. Predicted Hydrologic Effects of Pumping from the Lichterman Well Field in the Memphis Area, Tennessee. doi:10.3133/wsp1819B.

Ogletree, B.T., 2016. Geostatistical Analysis of the Water Table Aquifer in Shelby County, Tennessee. University of Memphis, Memphis, Tennessee.

Parks, W.S., 1990. Hydrogeology and Preliminary Assessment of the Potential for Contamination of the Memphis Aquifer in the Memphis Area, Tennessee. doi:10.3133/wri904092.

Parks, W.S. and J.K. Carmichael, 1990. Geology and Ground-Water Resources of the Memphis Sand in Western Tennessee. doi:10.3133/wri884182.

Parks, W.S. and J.E. Mirecki, 1994. Leachate Geochemistry at a Municipal Landfill, Memphis, Tennessee. Ground Water 32:390–398.

Pickett, R.E., 2012. Determination of Groundwater/Surface Water Interaction within a Sand Bottom Stream in West TN. The University of Memphis.

Rosenberry, D.O., 2008. A Seepage Meter Designed for Use in Flowing Water. Journal of Hydrology 359:118–130.

Rosenberry, D.O. and J.W. LaBaugh, 2008. Field Techniques for Estimating Water Fluxes Between Surface Water and Ground Water. doi:10.3133/tm4D2.

Schoefernacker, S., 2018. EVALUATION AND EVOLUTION OF A GROUNDWATER CONTAMINANT PLUME AT THE FORMER SHELBY COUNTY LANDFILL, MEMPHIS, TENNESSEE. University of Memphis.

Shaw, R.D. and E.E. Prepas, 1989. Anomalous, Short-Term Influx of Water into Seepage Meters. Limnology and Oceanography 34:1343–1351.

Shaw, R.D. and E.E. Prepas, 1990. Groundwater-Lake Interactions: I. Accuracy of Seepage Meter Estimates of Lake Seepage. Journal of Hydrology 119:105–120.

Silliman, S.E. and D.F. Booth, 1993. Analysis of Time-Series Measurements of Sediment Temperature for Identification of Gaining vs. Losing Portions of Juday Creek, Indiana. Journal of Hydrology 146:131–148.

Silliman, S.E., J. Ramirez, and R.L. McCabe, 1995. Quantifying Downflow through Creek Sediments Using Temperature Time Series: One-Dimensional Solution Incorporating Measured Surface Temperature. Journal of Hydrology 167:99–119.

Smith, M.R., 2018. Evaluating Modern Recharge to the Memphis Aquifer at the Lichterman Well Field, Memphis, Tennessee. University of Memphis.

Sophocleous, M., 2002. Interactions between Groundwater and Surface Water: The State of the Science. Hydrogeology Journal 10:52–67.

Van Arsdale, R., B. Waldron, N. Ramsey, S. Parrish, and R. Yates, 2003. Impact of River Channelization on Seismic Risk: Shelby County, Tennessee. Natural Hazards Review 4:2–11.

Villalpando-Vizcaíno, R., 2019. Development of a Numerical Multi-Layered Groundwater Model to Simulate Inter-Aquifer Water Exchange in Shelby County, Tennessee. University of Memphis.

Waldron, B.A., J.B. Harris, D. Larsen, and A. Pell, 2009. Mapping an Aquitard Breach Using Shear-Wave Seismic Reflection. Hydrogeology Journal 17:505–517.

Wang, L., W. Jiang, J. Song, X. Dou, H. Guo, S. Xu, G. Zhang, M. Wen, Y. Long, and Q. Li, 2017. Investigating Spatial Variability of Vertical Water Fluxes through the Streambed in Distinctive Stream Morphologies Using Temperature and Head DataEtude de La Variabilité Spatiale Des Flux Verticaux d'eau à Travers Le Lit d'une Rivière, Pour Différentes M. Hydrogeology Journal 25:1283–1299.

Winter, T.C., J.W. Harvey, O.L. Franke, and W.M. Alley, 1998. Ground Water and Surface Water; a Single Resource. doi:10.3133/cir1139.

Winter, T.C., J.W. LaBaugh, and D.O. Rosenberry, 1988. The Design and Use of a Hydraulic Potentiomanometer for Direct Measurement of Differences in Hydraulic Head between Groundwater and Surface Water. Limnology and Oceanography 33:1209–1214.

Woessner, W.W., 2000. Stream and Fluvial Plain Ground Water Interactions: Rescaling Hydrogeologic Thought. Groundwater 38:423–429.

Yates, R., B. Waldron, and R. Van Arsdale, 2003. Urban Effects on Flood Plain Natural Hazards: Wolf River, Tennessee, USA. Engineering Geology 70:1–15.